Astronomy & Astrophysics manuscript no. main
February 23, 2018

SimCADO - The Instrument Data Simulator for MICADO at the ELT

I. The imaging modes

K. Leschinski[1], O. Czoske[2,1], G. Verdoes Kleijn[3], W. Zeilinger[1], J. Alves[1], M. Mach[1], and S. Meingast[1]

[1] Department of Astrophysics, University of Vienna, Vienna, Austria
e-mail: kieran.leschinski@univie.ac.at
[2] Universität Innsbruck, Institut für Astro- und Teilchenphysik, Innsbruck, Austria
[3] Groningen University, Kapteyn Astronomical Institute, Groningen, The Netherlands
[4] Max Planck Institute for Extraterrestrial Physics, Garching, Germany

Received 01.03.2018; accepted TBD

ABSTRACT

Context. When the Extremely Large Telescope comes online at the end of 2024, MICADO will be the near infrared imaging camera available at first light. As part of the design activities for MICADO we have developed SimCADO: an instrument data simulator in the form of a Python package.
Aims. Here we describe the SimCADO software and the verification process with archival HAWK-I data. We also present some predications for detection limits and their corresponding distance limits for main sequence stars based on the current design of MICADO. The main aim of this study is to introduce the software and to provide these preliminary limits to the community to aid others in preparing science cases and observation strategies for MICADO and the ELT.
Methods. SimCADO produces simulated data frames for MICADO's 9 detector chip by applying the effects of each element along the optical train to a three dimensional (x,y,λ) description of the flux arriving from an astronomical object. The simulated images can be written to disk as FITS files and can be analysed by the standard suite of astronomical software. To verify the accuracy of SimCADO we generated descriptions of two globular clusters and used SimCADO to "observe" them. We then compared the characteristics of the simulated images with images from the ESO archive for the same clusters. We then used a model of the optical train for the current MICADO design to simulate observations of grids of stars in order to determine the sensitivity limits for MICADO at the ELT.
Results. SimCADO was able to accurately produce the image characteristics of raw archival HAWK-I data to within the limits of the model of the VLT/HAWK-I optical train. Using the current design of MICADO, SimCADO found detection limits in the J, H and Ks filters to be 28.7^m, 27.9^{m}and 27.3^{m}respectively for a 5σdetection in a 5 hour observation. This leads to the ability to detect individual A0 V stars at a distance of 4 Mpc (i.e. in Centaurus A), and M9 V stars in the Large Magellanic Cloud

1. Introduction

Over the next decade the era of the extremely large telescopes will be begin. The European Extremely Large Telescope (E-ELT) (Gilmozzi & Spyromilio 2007) will provide astronomers with the increase in resolution and sensitivity needed to solve many of the outstanding questions of modern day astronomy.

With a 39m primary mirror consisting of 798 [1] individually steerable 1.45m hexagonal mirror segments and a fully deformable quaternary mirror, the E-ELT will be capable of providing diffraction limited imaging. This corresponds to a core full width half maximum (FWHM) for the point spread function (PSF) in the J-band (~1.2μm) of ~8mas and ~14mas in the Ks-band (~2.16μm). Both single- and multi-conjugate modes for the adaptive optics will be possible. Six (four) laser guide stars (LGS) will be available to ensure that the E-ELT will always be able to provide AO-assisted observations.

As the first-light wide-field imaging camera for the E-ELT, MICADO - the **M**ulti-AO **I**maging **CA**mera for **D**eep **O**bservations (Davies et al. 2010) - will take advantage of the E-ELT's near-infrared optimised design to provide images at the diffraction limit. MICADO will provide a wide-field imaging mode and a zoom (narrow-field) mode with 4mas/pixel and 1.5mas/pixel plate-scales respectively. The detector plane will consist of nine 4096x4096 detector chips, allowing MICADO to cover a Field of View (FOV) of 55" by 50.5" in the wide-field mode and 20.5" by 19" in the zoom mode.

MICADO will also contain a series of additional modes, including: a long-slit spectrocgraphic mode with a spectral resolution of up to R~8000, windowed high-time-resolution (HTR) imaging mode with a read-out speed of up to 250 Hz and a high-contrast imaging mode.

As the scale and complexity of telescopes and instruments increases, so to does the importance of accurately being able to predict the performance of these systems. More and more emphasis is been placed on developing simulation software to model all aspects of new instruments before they enter the construction phase. As part of the development of the MICADO instrument, the MICADO Data Flow Systems work package has been tasked with creating a tool to simulate raw detector read-out images based on the current designs of the E-ELT and MICADO. Here we present SimCADO, the instrument data simulator for MICADO. SimCADO combines the most recent data from the other work packages in the consortium to allow the user to simulate the above mentioned raw data frames that will be produced by the E-ELT/MICADO optical system.

[1] Current data for the full E-ELT. This will change if ESO adopts the 2-phase approach for the construction of the telescope.

In this paper we will introduce the SimCADO package and show that it is a useful tool for producing accurate simulated images for the MICADO/E-ELT optical system. This paper is organised in the following way: 2 delves briefly into the motivation behind creating SimCADO as well as giving an overview of the scope of the project. The physical effects that SimCADO models are described in 3. A description of how we validated SimCADO by comparing simulated VLT/HAWK-I read-out frames to real images from the ESO archive can be found in 4 and predictions for the sensitivity of the MICADO/E-ELT system are presented in 5. A discussion of the results, assumptions and issues with the simulated images that SimCADO produces is presented for 6.

2. SimCADO - the Python package for simulating MICADO imagery

2.1. Motivation and Scope

The scientific return of instruments like the E-ELT and MICADO is the primary reason for building such complex pieces of machinery. Knowing in advance what the capabilities of an instrument will be, and preferably knowing just how well the instrument will perform for different configurations is invaluable during the design phase. Furthermore MICADO and other instruments like (e.g. HARMONI; Thatte et al. 2010, METIS; Brandl et al. 2008, etc.) are built by trans-national consortia, with many members from different institutes in different countries. As such the nodes in the consortia enjoy a certain level of geographic displacement. Each node in the consortia therefore often defaults to generating their own simulated data for the task to which they have been assigned. Additionally, the end users of the instrument also want to know how the instrument will behave and how useful it will be for their personal scientific projects well in advance so that they may prepare for when the instrument becomes available. All of these points can be considered true for almost all large instrument projects in modern day science - hence why there has been a very concerted effort by the scientific community, and very notably by the astronomical community to develop full scope instrument data simulators for major projects (see e.g. HSIM for HARMONI/EELT; Zieleniewski et al. 2015, the METIS/EELT simulator; Schmalzl et al. 2012, PhoSim for the LSST; Peterson et al. 2015, TOAD for 4MOST; Wi et al. 2014, WebbPSF for JWST; Perrin et al. 2015, IRIS Simulator for TMT; Wright et al. 2016, etc.).

2.2. The SimCADO audience

We have developed SimCADO over the last year for use primarily within the MICADO consortium, but also for interested external parties. SimCADO's main strength is that it gives all members of the consortium a common tool to generate simulated data for their assigned tasks. Among the consortium we see the main user groups being:

The science team: During the current design phase the science team members are running feasibility studies to determine which science cases are the biggest drivers for the design of the instrument. By using a common tool to generate simulated images, the science team, and those using the findings of the science team to make design decisions, can be confident that the results are all comparable.

The data reduction pipeline: In order to create a reliable set of reduced data product which are available from the beginning of operations, the data reduction pipeline must be developed before the first data are collected. SimCADO takes into account all processes which effect the incoming light as is travels from the source to the detector. As such it is perfect for generating so-called "dirty" images which can be used as fake input for the reduction pipeline. By using such images, the majority of coding for the reduction pipeline can happen without the need for the instrument to already be operational.

The data archive: The ability to produce simulated data also allows the development of a data archive to proceed prior to the availability of real data. SimCADO images will be used to help define the data products offered by MICADO and the method of storage and retrieval well before the instrument generates any images of it's own accord.

Instrument design team: SimCADO relies heavily on input from the different consortium work packages in order to produce images representative of the whole instrument. This in turn means that, by providing multiple sets of input data for a specific component in the optical train, a work package can use SimCADO to test the effect of different component designs on the final image quality. By using a standard set of science cases and weighting the importance of each aspect of the various science cases, trade-off analyses can be conducted. It should however be noted that SimCADO does **not** follow individual photons through the optical train. It assumes large numbers of photons and uses expectation values for photon intensities over the whole field of view. We therefore recommend that further investigation for design trade-offs should be undertaken with other more in-depth methods (e.g. ray-tracing) before any final decision is made.

Observation preparation software: Given the capabilities and expense of the E-ELT/MICADO system, observation time will be costly and in high demand. Therefore it is prudent to optimise observations to get the most out of any time on-sky. Currently exposure time calculators are provided to assist in observation preparation, however single numbers based on look up tables are often not enough to accurately predict exposure times given the myriad of celestial environments encountered during observations. For the E-ELT/MICADO system, integrating SimCADO into the preparation software will allow the user to not only determine the required exposure time length, but also to visualise and assess the effect of surrounding objects on the detectability of the target object. This should help to reduce the number of non-detections during actual observations, and therefore increase the scientific output of the MICADO and the E-ELT.

The MAORY consortium: MICADO will be the first and primary beneficiary of the MAORY AO module Diolaiti (2010). Consequently the development of the MAORY module is inextricable linked to MICADO. Design choices made in the MAORY consortium will have a direct impact on the quality of the science that MICADO will be able to produce. By using SimCADO, members of the MAORY consortium will also be able to see directly how these design choices will affect images produced by MICADO.

Astronomical community at large: Although first-light for the E-ELT is slated for 2024, preparation work needs to begin well in advance so that the astronomical community can "hit the ground running" once the E-ELT and MICADO are online. Many of the ideas that will be tested post-2024 will need be developed over the coming years. It is therefore important that the astronomical community have a tool that enables new ideas to be thoroughly tested, and where necessary preliminary observations to be conducted, before applying for time with MICADO. SimCADO will help when testing the feasibility of observations for new ideas.

2.3. SimCADO as an Instrument Data Simulator

First an foremost SimCADO was conceived as an instrument data simulator (IDS), not an end-to-end (E2E) simulator. An IDS is different from an E2E simulator in the follow way: an E2E simulator models the interactions between each object and each element in the optical train with the incoming photons in a physically realistic manner, i.e. taking into account the physical interactions between photons and computer representations of physical objects along the optical train (see photon-tracing in PhoSim for the LSST Peterson et al. (2015)). An IDS on the other hand, turns the effects of each element in the optical train into mathematical operators, which are then applied to an input "image" (a 2D/3D representation of the sky). IDSs require much less computation power and are therefore much better suited for quick, personalised simulations and prototyping. However this comes at the cost of flexibility. E2E simulations can create images for any physical configuration of the optical train, as long as a physical model of all components exist in memory. IDSs only generate output for a certain configuration if data (often originally created by an E2E simulation) already exists and can be converted into a series of mathematical operators. A good example is the case of the PSF. Given a point source with a certain brightness, the PSF will appear on the focal plane of an E2E simulation by only supplying a model of the physical objects along the light's path (spiders, mirrors, pupil stops, etc). An E2E simulator needs only the values pertaining to the physical positions and dimensions of these objects. An IDS on the other hand is able to project a PSF onto the focal plane because a mathematical description (either a 2D image array or a 2D function) of that PSF has been supplied. The IDS then convolves this description with the point source. Regardless of how the optical train changes, unless this mathematical description has been updated from another source (i.e. output from an seperate E2E simulator) the IDS images will continue to display the same PSF.

The main advantage of developing and using an instrument data simulator lies in its speed and ease of use. Because IDSs rely on the results of other simulations, IDS simulations are many orders of magnitude faster than those conducted with E2E simulators. Our main goal with SimCADO was to provide a tool which gives the casual user the ability to simulate images for MICADO in a matter of minutes on their own laptop. Such an approach is advantageous to both the user and the developer compared to the alternative model whereby the user must submit a simulations request to a dedicated "simulations" team. With SimCADO running on the users laptop, both the time the user must wait for results and the work load of the simulations team are drastically reduced. This in turn allows the simulations team to direct their efforts towards improving the software and keeping the instrument configuration up to date.

Further justification for concentrating our efforts on an IDS rather than an E2E package comes from the fact that for the majority of cases, the optical train stays exactly the same. Therefore there is no need to re-simulate from scratch each and every photon interaction simulated by the E2E approach every time a simulation is run.

3. The physical effects modelled by SimCADO

SimCADO takes into account all effects between the light source and the detector. This includes the atmosphere, the telescope, the MICADO instrument, and the detector array. We have designed SimCADO is such a way as to allow any optical train to be modelled, providing all the relevant data is available [2] The default configuration is for the E-ELT/MICADO optical train. For testing purposes we have implemented a variation of SimCADO that reproduces the effects of the VLT/HAWK-I optical train (see section 4). In this section we describe the effects of the optical elements which the current version (0.4) of SimCADO takes into account.

For a full description and discussion of the internal workings of the SimCADO package, the reader is directed to the paper by Leschinski et al. (2016) and to the online SimCADO documentation: `www.univie.ac.at/simcado`.

3.1. Atmosphere

Transmission and Emission

The SkyCalc tool [3] (Noll et al. 2012; Jones et al. 2013) provides accurate spectral models of the atmospheric transmission and emission (see 3.1 for the transmission and emission curves). For SimCADO we have taken the default model, which uses atmospheric conditions averaged over the whole year and a unity airmass. In a future release we hope to include the functionality to query the SkyCalc server directly from within SimCADO. However until such time, if the user is interested in investigating the effects of different atmospheric conditions on the resulting detector output, SimCADO accepts FITS files generated by the online SkyCalc tool as input for simulation runs.

As an alternative to using the default spectral energy distribution provided by SkyCalc, the user may instruct SimCADO to use a broadband magnitude to model the sky background emission. The number of photons are calculated from a spectrum of Vega multiplied by the transmission curve for the given broadband filter and scaled according to the user's sky background surface brightness.

Atmospheric diffraction

For effects which act along all three relevant simulation dimensions (x, y, λ) SimCADO uses an adaptive layered approach. Briefly this means that SimCADO determines how separated in spectral space two individual monochromatic images can be before a noticeable spatial shift between two adjoining layers occurs. This parameter can be set in the SimCADO configuration file. By default a new spectral bin is created once the shift due to the atmospheric dispersion is greater than one pixel (i.e. 4mas and 1.5mas in the wide-field and zoom modes respectively). The spatial shifts induced by the atmosphere are calculated according to the formulae from Stone (1996) and from the review by Pedraz [4]. In order to avoid unnecessarily increasing the computational workload, any shifts induced by the atmospheric dispersion are inversely scaled according to the performance parameter for the atmospheric dispersion corrector (ADC) (which by default is set to 100% - i.e no dispersion at all).

PSF variability

SimCADO does not create atmospheric point speread funtions (PSFs) on the fly. Instead it requires a PSF to be provided, either by the other teams working in conjuction with the MICADO consortium (i.e. the SCAO and MCAO simulation teams) or by the user. PSFs will be discussed in greater detail in section 3.2 however it is worth mentioning here that SimCADO pro-

[2] We have also created configuration packages for the HST+WFC3 systen and the NTT+SOFI system.

[3] `https://www.eso.org/observing/etc/bin/gen/form?INS.MODE=swspectr+INS.NAME=SKYCALC`

[4] `http://www.caha.es/newsletter/news03b/pedraz/newslet.html`

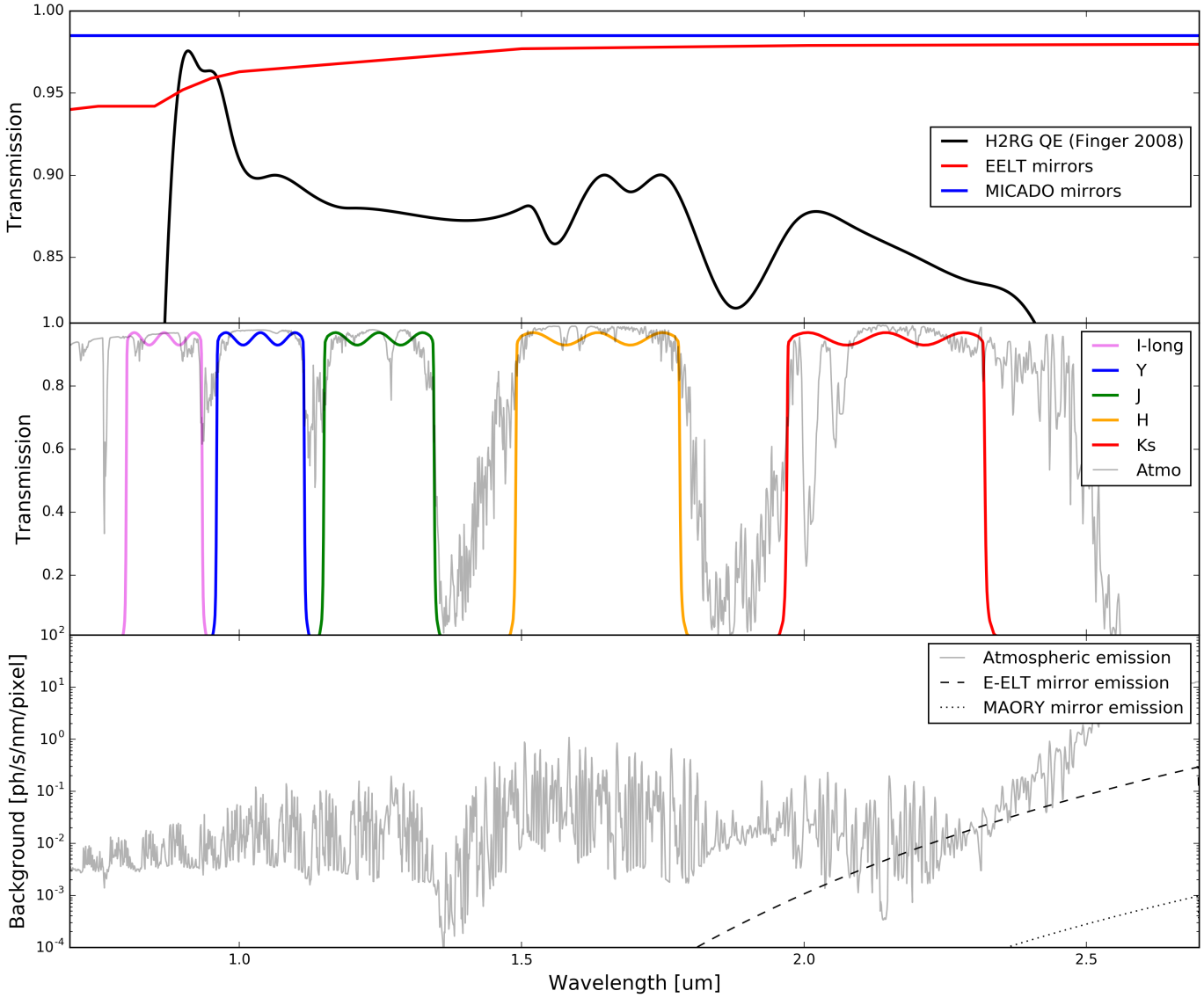

Fig. 1. Default transmission and emission curves used by SimCADO. Top: The mirror transmission curves for both the E-ELT (warm optics) and MICADO (cold optics) plotted together with the quantum efficiency (QE) curve for the HAWAII 2RG detectors. The E-ELT will use a AgAl mirror coating with a MgF2 protective layer (Boccas et al. 2006) while the 14 MICADO mirrors will be gold coated (Davies et al. 2016). SimCADO uses the QE curve for the H2RG detectors because information on the H4RG detectors is not currently available to the public. As soon as the QE curve for the 4k detectors becomes available, the SimCADO defaults will be updated. Middle: A selection of broadband filters for MICADO (IYJHKs) based on the HAWK-I filter set. The selection of narrow band filters has not yet been decided and so none are shown here. SimCADO does ship with a collection of curves for the most common narrow band filters. The atmospheric transmission curve used by SimCADO was generated by the skycalc tool (Noll et al. 2012; Jones et al. 2013) and can be adjusted for zenith distance. Bottom: the photon background flux per MICADO wide-field mode pixel (i.e. 4mas) coming from the atmosphere and from the E-ELT and MAORY mirror greybody emission. The units are in photons per second per nanometer calculated for the full area of the E-ELT's mirrors. The sky background emission spectrum was generated using the skycalc tool with the default parameters. The E-ELT mirror emission is for an ambient dome temperature of 0 degrees Celcius and combines the emission from all five of the E-ELT's mirrors. The MAORY mirror emission is assuming warm optics at the dome temperature and the optical train as detailed by Diolaiti (2010) and Diolaiti et al. (2016). The total area of the MAORY mirrors is taken to be ~3.4m^2

vides a series of functions for generating "E-ELT" PSFs based on the POPPY PSF simulation package (Perrin et al. 2015). The function `simcado.psf.poppy_ao_psf()` allows the user to specify the level to which the seeing halo is added to an ideal diffraction limited PSF, thus allowing the user to create PSFs for different seeing conditions.

Currently SimCADO doesn't automatically include time variability in the PSF or in the atmospheric parameters. However, SimCADO's implementation in Python allows the user to script many different simulation configurations, thus providing the functionality to implement temporally varying atmospheric conditions. An automated method for doing this is foreseen for later releases of SimCADO.

3.2. The E-ELT

Point Spread Function: Being an IDS, SimCADO doesn't need to know how the PSF is generated or what happened to it before

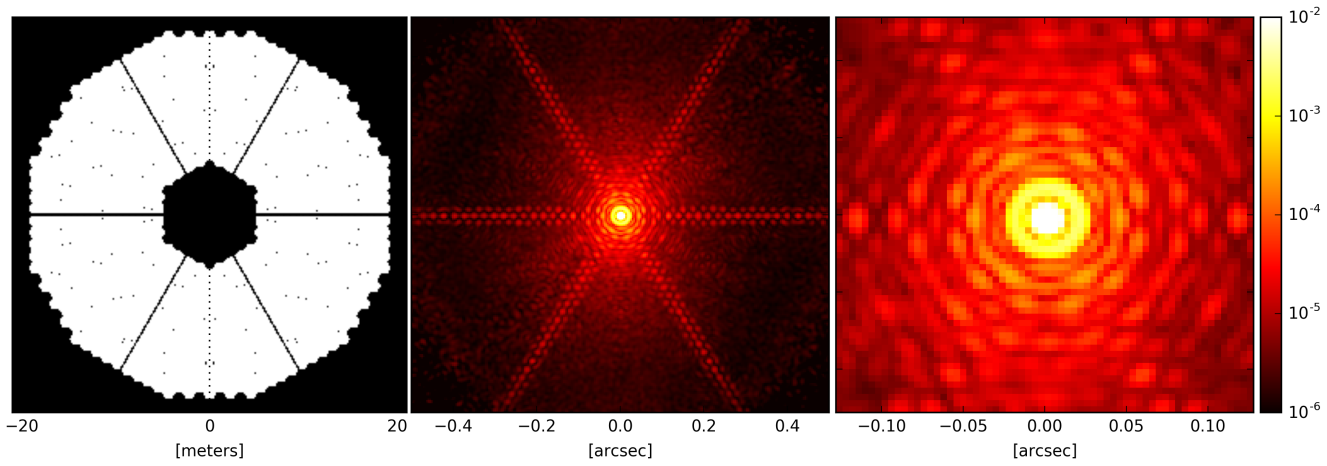

Fig. 2. Left: the E-ELT pupil at first light for each of the single-phase (top) and double-phase (bottom) mirror configuration options, not taking into account any circular obscurations in the pupil plane. For the option of a two-phase approach, only 588 of the 798 mirrors will be installed in M1. The five inner rings will be installed during the second phase of the project. Middle: the analytical PSF for a Strehl ratio of 50% in Ks band over a 4" FoV for an ideal E-ELT optical train for each of the two construction plans as generated by SimCADO and POPPY. Right: a cutout of the central 0.128öf the PSFs. The increased flux in the higher order Airy rings is quite noticeable when the inner five rings are missing from the primary mirror. The PSFs shown in the middle and right columns are with an extra circular pupil which removes the effect of the straight inner and outer edges of the hexagonal segments of the primary mirror.

the instrumental focal plane. All SimCADO needs is the total (wavelength dependent) effect of the whole optical train on the spatial distribution of light on the focal plane. How the atmosphere deforms the PSF and how the AO modules correct for this are outside the scope of SimCADO. Only the net effect of the two counteracting operations are important for simulations.

Currently the two adaptive optics (AO) modes that will be offered with MICADO are:

- single conjugate (SCAO) (Clénet et al. 2016), which will provide diffraction limited imaging over a 3" field of view with strehl ratios of >60%
- multi-conjugate (MCAO) in conjuction with the MAORY module, which will provide diffraction limited imaging of the full MICADO field of view with strehl ratios between 30% and 50% in Ks band (Diolaiti et al. 2016)

Currently SimCADO only provides a SCAO PSFs from the E2E simulation efforts of Clénet et al. (2015) (obtained via private communication). MCAO PSFs will be included as soon as the MAORY consortium releases them for public use. Currently the PSFs do not take into account variability over the FoV. This effect will be included in a later release of the simulator.

In addition to the PSFs provided by the E2E AO simulations, SimCADO also provides functionality to generate lower fidelity PSFs using an analytical model. This model is not as accurate as the E2E simulations but it does allow the user to conduct comparative studies. For example the user can investigate how different Strehl ratios will affect the results for a certain science case. The analytical PSF is generated by summing two weighted PSFs - a diffraction limited PSF and a Seeing limited PSF - according to the equation:

$$PSF_{(Analytical)} = SR \times PSF_{(Diffraction)} + (1 - SR) \times PSF_{(Seeing)} \quad (1)$$

where SR is the desired Strehl ratio, $PSF_{(Diffraction)}$ is the diffraction limited PSF generated by the POPPY package (Perrin et al. 2015) for a 39m diameter segmented mirror with six support beams for the secondary mirror (see 3.2), and $PSF_{(Seeing)}$ is a PSF following a Moffat profile with a full width half maximum (FWHM) corresponding to the seeing limit of the observations. Both primary mirror configurations for ESO's single-phase and double-phase construction proposals are available to the user. For the Seeing limited PSF, SimCADO uses a FWHM of 0.8". The default Strehl ratio for the analytical PSF is set to the Strehl ratio that MAORY is required to provide, i.e. 30% in K band and 12% in J band (Diolaiti et al. 2016).

****Put something about the spatial/spectral changes to the PSF, i.e. changes of the field of view and with wavelength****

Transmission and emission: SimCADO uses the reflectivity curve provided by the ESO Data Reference Mission (DRM) for the E-ELT [5] for an aluminium silver mirror coating with a magnesium flouride protective layer (AgAl-MgF2). This is currently the preferred mirror coating for all five of the E-ELT mirrors. For comparison, SimCADO also provides the transmission curve for a pure aluminium coating (as used at the VLT). The reflectivity in the near infrared regime is almost constant at ~98%.

The grey-body emission for the E-ELT is calculated by assuming all emission is coming from a single surface with the combined area of all five mirrors (~1030m^2) and at a temperature of 0 degrees Celcius. This light is subject to the transmission losses of all five E-ELT mirrors. While this isn't a completely correct representation of what happens to the grey-body emission - light from M1 is subject to reflectivity losses from 4 mirrors, while there is no loss of emitted light from M5 due to E-ELT surfaces - because of the shear size of M1 (~980m^2) the difference in total grey-body light from the five E-ELT mirrors is < 0.15%. This source of uncertainty is far outweighed by the uncertainty in the assumed temperature of the mirrors. The increase in computation speed by only using one characteristic transmission curve for the grey-body emission is noticeable and justifies this approximation.

Wavelength independent spatial effects: Effects related to unwanted movements of the telescope are also built into SimCADO. Wind jitter and vibrations due to the cooling equipment introduce a further blurring term into the image. This can be

[5] https://www.eso.org/sci/facilities/eelt/science/drm/

Wavefront error rms [nm]	Surfaces	Material	Optical element
20	11	gold	Mirror
10	4	glass	Entrance window
10	2	glass	Filter
10	8	glass	ADC

Table 1. The root-mean-square wavefront error expected for each surface in the MICADO optical train. The total wave front error is expected to be on the order of 76 nm which translates to a decrease in PSF peak strength of ∼5% at 2.2um ∼14% at 1.25um (R. Davies, private communication)

modelled by convolving the final focal plane image with a 2D Gaussian distribution. The FWHM of the Gaussian is a function of the strength and frequency spectrum of both the vibrations and the wind. At this stage we have assumed that the E-ELT's vibration dampening mechanisms will remove the vast majority of vibrations. As such SimCADO defaults to a FWHM of <0.004", thus removing this effect from the default simulations.

SimCADO provides the functionality to simulate the smear introduced by sub-optimal mechanical performance of the E-ELT's tracking system. However a quick back-of-the-envelope calculation shows that the update frequency of the E-ELT's stepper motors needs to be on the order of 10-100 KHz if the sky is to move less than a MICADO pixel length between updates. This is well within the scope of modern day stepper motor technology and so by default SimCADO assumes that the E-ELT's tracking system will not cause noticeable image smearing.

3.3. MICADO

We have developed SimCADO during the design phase of MICADO. While the core API of the package do not change, the default configuration for SimCADO is continually updated to reflect the most recent design of the instrument. Values presented in this subsection are correct at the time of publishing, however may not be identical to those in the most recent version of the SimCADO package. See Davies et al. (2016) for the MICADO design at the time of writing.

Transmission: SimCADO takes into account all optical surfaces along the instrument optical train including: the cryostat entrance window (4 surfaces), the internal fold mirrors, the atmospheric dispersion corrector (4 prisms, 8 surfaces), the zoom optics, the filters (2 surfaces) and the pupil placeholders. Additional surfaces needed for the spectroscopy mode include the entrance slit and the grisms. These will described in a companion paper on the SimCADO spectroscopy mode.

Currently by default all the mirrors are coated with gold and have a reflectivity of 98.5% across the whole spectral range. SimCADO also ships with all common visual and NIR broadband filters (UBVRIzYJHKKs) and a series of common narrow band filters for NIR observations, taken from the spanish virtual observatory database [6]. The user is also able to direct SimCADO to use any filter curve for which they have an ASCII file containing wavelength and transmission values using the `TransmissionCurve` object.

Non Common Path Aberrations (NCPAs): The default PSFs do not take into account the NCPAs due to the difference in optical path to the wave-front sensors and to the detector array. Characterising the MICADO NCPAs is still an active topic of discussion. We will include both the spatial and spectral effects of the NCPAs in a later release of SimCADO once a model exists to describe them. In the mean time we are able to use wave-front error budgets to determine an approximate wavelength dependent reduction, f_{peak}, in the peak intensity of the PSF due to the NCPAs according to equation 2:

$$f_{(peak)} = e^{-(2\pi WFE_{total}/\lambda)^2} \quad (2)$$

where WFE_{total} is the total wavefront error expected for all NCPAs along the MICADO optical path and λ is the wavelength for which the PSF has been constructed. Table 3.3 details the individual wavefront errors that SimCADO uses to calculate WFE_{total}. The total wave front error is expected to be on the order of 76 nm which translates to a decrease in PSF peak strength of ∼5% at 2.2um ∼14% at 1.25μm (R. Davies, private communication).

Atmospheric Dispersion Corrector (ADC): Like the PSF, the effect of atmospheric dispersion is visible in all three instrumental dimensions (x, y, λ). In order to simulate this effect SimCADO creates a series of monochromatic image slices for a series of spectral bins within the filter wavelength range (see Leschinski et al. 2016 for a detailed description of how SimCADO does this). The bin width is chosen in such a way that the elongation induced by the atmospheric dispersion is never greater than one pixel (i.e. 4mas in wide field mode, or 1.5mas in zoom mode). If the ADC is working perfectly then the atmospheric dispersion is completely removed and the spectral bin width is equal to the full width of the filter. If the ADC is turned off, the relative shift of an image over the full J-band is around 0.19", or almost 50 wide-field pixels, at a zenith distance of 60 degrees. To maintain a relative shift per monochromatic image slice of less than a single pixel, SimCADO must generate almost 50 monochromatic slices, each shifted relative to the reddest slice. By stacking all the slices (including shifts) on the detector plane the dispersion caused by the atmosphere can be reproduced in the final output image. By default SimCADO assumes that the ADC is working perfectly and so doesn't need to introduce any extra image slices. Once the design of the ADC progresses and the residuals of the correction are quantified, we will update the default parameters for SimCADO to reflect this. **See [**Navaro**] for a more detailed description of the ADC.**

Derotator: A perfectly functioning derotator is essential for maintaining the astrometric accuracy of sources near the edges of the detector plane. Similar to the ADC we have implemented the effect of a less-than-perfect derotation by combining a series of image slices for which the shift at the edge of the detector array is less than one pixel. However as the sky rotation is a purely spatial effect, the images slices are generated for temporal bins (i.e. a series of short "exposures"), as opposed to the spectral bins for the ADC (again, see Leschinski et al. 2016 for further details). By default SimCADO assumes perfect derotation, however as always the defaults will be updated as soon as more information becomes available.

Instrumental Distortion: Another effect that is important for accurate astrometric measurements is the instrumental distortion. Although not included in the publicly available version of SimCADO at the time of writing (version 0.4) this functionality is currently being developed and will be included in future releases of the package. The implementation of the instrumental distortion will be discussed in a companion paper detailing the astrometric capabilities of MICADO and SimCADO.

[6] `http://svo2.cab.inta-csic.es/theory/fps3/index.php?mode=browse`

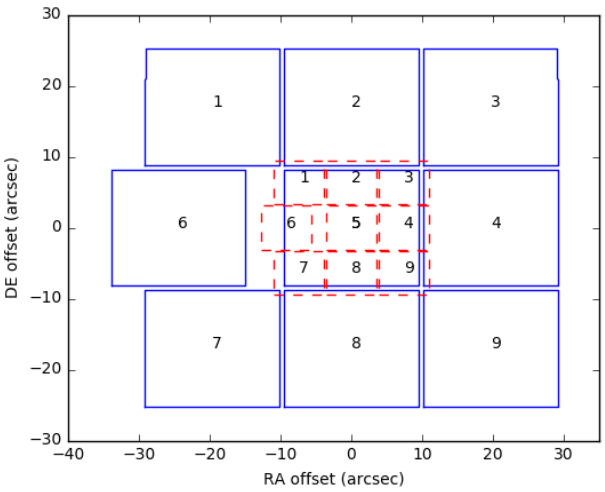

Fig. 3. The footprints of the two imaging modes for MICADO. The wide-field mode (solid lines) has an on-sky footprint of *sim*55"*times*50', while the zoom mode (dashed lines) has an on-sky footprint of *sim*20.5"*times*18.75". The H4RG will only be 3-side buttable due to the placement of the read-out electronics, the result of which is the extended gap between chips 3 and 4 in the middle row.

3.4. MICADO Detector Array

The current design for MICADO includes a 3x3 array of HAWAII-4RG chips (Davies et al. 2016). SimCADO takes into account the positions of the chips on the focal plane as well as the gaps between the nine chips, the electronic noise characteristics of the HAWAII chips as well as the linearity of the chips. Most of this information is not publicly available and so we have based the detector characteristics primarily on the H2RG chips, the predecessors to the H4RGs.

Electronic noise: Rauscher (2015) created the python package NGHxRG [7] to simulate read noise frames for the HAWAII-2RG detectors used in the JWST NIRSpec instrument (Posselt et al. 2004). SimCADO uses this package to create noise frames for the HAWAII-4RG detector series. Included in the noise frames are: white (read) noise, residual bias drifts, pink 1/f noise and alternating column noise. Picture frame noise can also be included, however as there aren't yet any estimates for MICADO, SimCADO bases it's picture frame noise on the default file provided by the NGHxRG package. **??** shows the default parameters used when generating the noise frames.

Detector gaps: In it's base configuration, the MICADO detector plane will consist of 9 H4RG detectors, each covering slightly more than 16"*times*16" on sky. Because of the read out electronics, each chip will only be 3-side buttable, meaning that one of the eight outer chips must be placed further from the central chip that its counterparts. This can be seen in on-sky footprints of the zoom and wide-field modes in figure 3.4. SimCADO contains configuration files detailing the positions of the detector chips for each of these base modes. Due to the way SimCADO was built, any configuration of detectors is possible as long as the user specifies the centre of the chips relative to the centre of the field of view and the pixel-dimensions of the chips. This feature is also useful for simulating the windowed read-out functionality of the H4RG chips.

Linearity, Saturation, Persistence and Cross-Talk: Because data on the H4RG aren't yet publicly available, we have assumed that the chips will have a similar performance to the H2RG chips which are found in many current NIR instruments (e.g. VLT/HAWK-I, JWST/NIRSpec). The data for the linearity curve and saturation limits have therefore been taken from the HAWK-I detector array. As persistence and pixel cross-talk are more complex to model, SimCADO does not currently simulate these two effects. We do however plan to implement them in a later version of SimCADO.

Read out schemes: SimCADO has two functions for reading out the chips on the detector array: "non-destructive" and "super-fast". The non-destructive mode mimics the functionality of the HAWAII 2RG chips, which allows the user to measure the pixel values without actually destroying the content of the pixels. This mode allows any non-destructive read-out scheme to be implemented, including the commonly used Fowler, Double-correlated or up-the-ramp schemes. However, this mode is not the default and the scheme must redefined by the user.

The default read-out scheme for SimCADO is the so-called "super-fast" mode. This uses a simple implementation of the standard signal-to-noise equation, expanded to a two-dimensional image. Because the majority of observations are normally background limited and not detector noise limited, the "super-fast" mode therefore does not co-add a series of single exposures, but rather creates an single read-out with an exposure time equal to the duration of the full observations (i.e. `EXPTIME = NDIT*DIT`). Shot noise in the image scales a the square root of the total observation time. It is no surprise that the super-fast mode is NDIT times faster than the non-destructive read-out mode. For observations using super-fast which are greater than 10 minutes, we recommend "turning off" SimCADO's detector linearity functionality so that the signal increases linearly to exposure time over the full duration of the observation. In future releases this will occur automatically based on the chosen mode. [8]

3.5. On whom does SimCADO depend for the data

Because SimCADO is an IDS, the package relies on data generated by other working groups that describe the optical effects present in the system which SimCADO simulates. As the development of MICADO is still a work in progress, we are continually updating the internal data sets as the new data becomes available.

Put in a table here detailing the critical data sets

4. Validating SimCADO with raw HAWK-I data

Aside from testing during the coding phase, we tested the accuracy of SimCADO by comparing simulated raw detector read-out images to real raw observations from HAWK-I at the VLT. HAWK-I, the High Acuity Wide-field K-band Imager, (Kissler-Patig et al. 2008) is a present-day analogue to MICADO's imaging modes and thus a good test-bed for these comparisons. We created a configuration file that reflected the VLT+HAWK-I optical train and used a combination of the instruments data publically available on the ESO website [9] and HAWK-I calibration

[7] http://jwst.nasa.gov/resources/nghxrg.tar.gz

[8] It should be noted that regardless of the status of the detector linearity, there is still a hard limit of 2.14E9 photons per pixel set by numpy's "poisson" function. Larger values raise an error message. Hence all pixel values above 2.14×10^9 are capped so that shot noise can still be applied to the image.

[9] `http://www.eso.org/sci/facilities/paranal/instruments/hawki.html`

data from the ESO archive to create a version of SimCADO that simulates raw observations from HAWK-I. We then compared the photometry of stars in both the raw HAWK-I and simulated SimCADO images to gauge the accuracy of the simulations.

4.1. Modelling HAWK-I with SimCADO

To create a model of the HAWKI optical train, SimCADO required the following data:

- an estimate of the Point Spread Function (PSF) for the whole VLT/HAWKI system,
- transmission/reflectivity curves for each fo the surfaces along the optical path,
- details of the HAWKII-2RG detector characteristics and,
- a set of observational conditions.

The PSF: The previous lack of an adaptive optics system in the VLT+HAWK-I optical train greatly simplified simulations. The combined system PSF could be, to a very good approximation, described by a 2D diffraction limited Moffat profile due to the round monolithic mirrors of the VLT (Dierickx et al. 1990) and the seeing limited nature of the observations. To include the effect of the "spiders" that are part of the support structure for the secondary mirror, we used the POPPY package to generate a diffraction limited PSF for an 8.2m circular aperture with a 1.1m secondary obscuration and 4x 0.1m support beams. We then convolved this diffraction limited PSF with a 0.5" Gaussian to mimic the Seeing-limited nature of HAWKI observations.

Transmission along the optical train: The combined optical train of HAWKI and the VLT's UT-4 contains 7 aluminium-coated mirrors, an entrance window, a series of standard NIR filters and a detector plane with 4 HAWKII-2RG chips. The transmission, reflectivity and quantum efficiency curves for each of these elements were obtained and combined in SimCADO. The resulting transmission curve had an average transmission value of 0.52, which is very similar to the value assumed by the online exposure time calculator provided by ESO. [10]

The detector array: Four HAWKII-2RG chip (Loose et al. 2007) are used in HAWK-I, each with its own unique characteristics. To general detector noise was generated internally by SimCADO, using the NGHxRG package (Rauscher 2015). The quantum efficiency curve was taken from Finger et al. (2008). A low resolution custom linearity curve for the detectors was included. The curve was determined by fitting Gaussian profiles to the wings of a series of saturated stars in the raw observations and comparing the theoretical height of the best-fit Gaussian profile to the actual pixel value in saturated regions. A plate scale of 0.106" was also used by SimCADO.

Instrumental distortion was neglected because its effect was minimal when determining the photometric accuracy of a simulated stellar field. The flat field effect of the whole system was also neglected for this study. This was under the assumption that it will not drastically affect the photometric accuracy of the majority of stars in any simulated field.

It should be noted that we are in the process of conducting a further study to quantify the extend to which different atmospheric conditions affect the accuracy of images generated with SimCADO. For this study we were granted 5 hours of technical time on HAWK-I. The results of this study will be published in a companion paper.

[10] `https://www.eso.org/observing/etc/bin/simu/hawki`

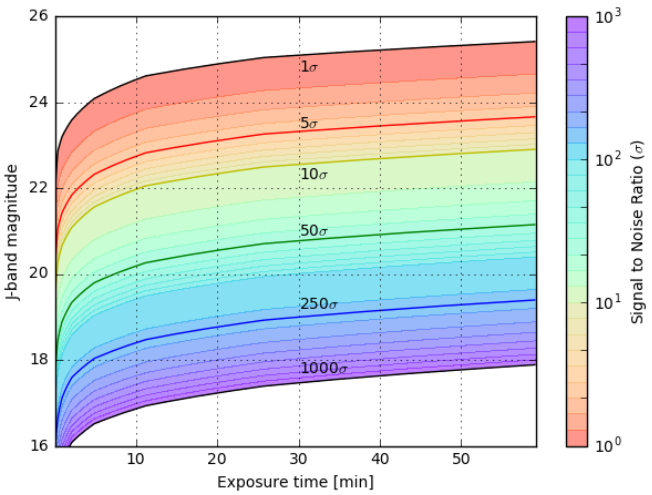

Fig. 4. A grid of hundred stars were observed for different durations between 1 and 60 minutes using SimCADO configured to model the UT4/HAWKI optical system. The 5σcontour in this graph is very similar to the theoretical 5σdetection limit returned by the ESO HAWKI ETC. The one hour 5σmagnitude limit ($J = 23.7^m$) also agrees well with the sensitivity limits published by Kissler-Patig et al. (2008).

4.2. HAWKI-I Sensitivity with SimCADO

As a first test we compared the limiting magnitudes of images generated with SimCADO to both the limiting magnitudes given in the HAWK-I user manual, and those given by the exposure time calculator (ETC) on the ESO website. Table **??** shows that the limiting magnitudes for SimCADO in the J, H, K and Brγfilters compares very favourably with the data provided by the ESO exposure time caluclator. The observation parameters used in SimCADO were set to be identical to those described in the HAWK-I User Manual, namely: Seeing of 0.8" in V-band and an Airmass of 1.2. Figure 4.2 shows the evolution of several relevant detection limits (e.g. 5$\sigma$for photometry, ~250$\sigma$for astrometry) for HAWK-I as determined by SimCADO.

4.3. Comparison of SimCADO images with real observations

To test how well SimCADO reproduces the spatial aspects of an observation, we downloaded four raw FITS files for the popular globular clusters M4 and NGC4147 from three different observing runs conducted between 2007 and 2015 from the ESO archive. Table 4.3 lists the main parameters of these observations. Globular clusters by virtue of their age contain very little gas or dust and hence essentially no star formation activity. This makes them easy objects to model. We chose this series of raw images to test the performance of SimCADO over multiple observing configurations.

In order to simulate the raw images we generated SimCADO-readable `source` objects for the gobular clusters M4 and NGC4147 using the 2MASS RA, Dec positions and apparent magnitudes of all sources in the resepctive HAWK-I field of views. These `source`-objects were fed into the SimCADO model of HAWK-I and the `Detector` module was read-out. The resulting images were analogues of the raw images generated by the HAWAII-2RG chips inside HAWK-I. They contained raw pixel data (in ADUs) as delivered by the read-out electronics of the HAWKI detector array. We used aperture photometry to determine the total flux of each star and then compared flux values to the theoretical fluxes calculated from the 2MASS magnitudes.

Filter	Exposure time	SimCADO	ETC	Kissler-Patig (2008)
J	1 hr	23.7^m	24.2^m	23.9^m
	1 min	21.4^m	22.0^m	
	2 sec	19.7^m	20.1^m	
H	1 hr	22.7^m	23.3^m	22.5^m
	1 min	20.5^m	21.0^m	
	2 sec	18.7^m	19.2^m	
Ks	1 hr	21.9^m	22.2^m	22.3^m
	1 min	19.7^m	19.9^m	
	2 sec	17.8^m	18.1^m	
Brγ	1 hr	21.6^m	20.9^m	
	1 min	19.5^m	18.7^m	
	2 sec	17.5^m	16.8^m	

Table 2. Limiting magnitudes calculated for HAWK-I from images generated by SimCADO, the ESO ETC and taken from the HAWK-I User Manual. The SimCADO limiting magnitudes were calculated based on a 5σdetection in a grid of 100 stars with magnitudes spread linearly between $14^m$and 27^min the respective filters. The FWHM for the SimCADO PSF was chosen to match the "Image Quality" parameter given by the ETC. For a Seeing value of 0.8" in V band and an Airmass of 1.2, the resulting FWHM for J, H and Ks (Brγ) band respectively was 0.62", 0.58", 0.53"

ESO archive filename	Filter	Exposure [s]	V-band Seeing [arcsec]	Airmass	Object
HAWKI.2015-06-10T05_12_28.683.fits	Ks	10	0.9	1.05	M 4
HAWKI.2007-08-05T01_34_45.908.fits	Ks	10	NA	1.05	M 4
HAWKI.2007-08-05T23_14_33.748.fits	J	10	1.1	1.02	M 4
HAWKI.2014-01-19T07_49_48.826.fits	J	2	0.74	1.44	NGC 4157

Table 3. The raw HAWK-I data from the ESO archive used in this study. The three observations of M4 were used to test the photometric accuracy of SimCADO under the assumption that the background level should remain similar. The observation of NGC4147 was used to test the background flux under a different exposure lengths.

As was to be expected, the SimCADO fluxes were in excellent agreement with the 2MASS fluxes (Fig. 4.3. This was to be expected as the 2MASS catalogue provided the input for the SimCADO source model. Although figure 4.3 shows a dependent correlation between the two axes, we have included this figure to show the reliability of SimCADO when propagating flux. As long as the input data is accurate, SimCADO will faithfully reproduce the source flux in the form of pixel counts in the detector electronics. The deviation from the one-to-one line in figure 4.3 is due to a combination of two factors: SimCADO recreating the non-linearity of the HAWAII-2RG detectors for pixel count higher than ~100,000, as well as the background annulus used in the aperture photometry being too small for the brightest stars. While an adjustable size for the annulus would have slightly improved the comparison, it wasn't deemed necessary to illustrate SimCADOs ability to accurately propagate flux through the optical train.

The same aperture photometry method was also applied to the raw HAWK-I images from the archive. Figure 4.3 shows a comparison between the total aperture flux for stars in a real K-band image of M4 and it's simulated counterpart. There is a good correlation between the fluxes extracted from the two images.For each chips 1 and 2 >75% of stars with A-grade 2MASS photometry fall within these bands. For chips 3 and 4 this figure is >85%. ~55% of the sources with C-grade or less photometry flags fell outside the ±30% bands. When investigating these sources we found a large fraction to be single entries in the 2MASS catalogue which were resolved out into two stars in the HAWK-I images. Hence the scatter seen in figure 4.3 is primarily due to the faint background sources contaminating the photometric measurements. As the artificial globular cluster for SimCADO is based on the 2MASS catalogue for M4, there are no sources fainter than the 2MASS detection limit. The presence of the fainter background sources in the real images greatly reduced the accuracy of the flux measurements for sources with magnitudes Ks>12^m. In this faint regime "hot" or "dead" pixels also affect the accuracy of the photometry. As we did not provide SimCADO with a pixel map for HAWK-I, malfunctioning pixels included in the simulated images were not the same as those on the HAWK-I detectors. Finally the small but uniform <0.1^mshift in the photometry between detector chips was caused by a combination of the inhomogeneity of the detector gain factors (Kissler-Patig et al. 2008).

Aside from reproducing the photometric characteristics of stars on the detector plane, and more important for making predictions for MICADO and the ELT, is SimCADO's ability to accurately reproduce the background flux distribution. As there was no information readily available for the strength of the sky background for the raw archive images, we assumed standard sky background magnitudes as given by Cuby et al. (2000). This assumption was adequate for SimCADO to reproduce the shape of the flux histogram as shown in Figure 4.3. It should be noted that the sky background varied between the 3 sets of archival data. This resulted in background fluxes from SimCADO being ~0.1^mlower than the backgrounds in the raw J and Ks images from the 2007 observations of M4. For the other observations, the simulated images had background fluxes on the order or ~0.4^mfainter than in the raw HAWK-I images. Given that Moreels et al. (2008a) reports that NIR sky backgrounds can vary up to 0.75^mper night, we concluded that this difference was due to the observational conditions. The observation of NGC4147 was taken at an Airmass of 1.44, while the 2015 observation of M4 was conducted under "clear" conditions, as defined by ESO [11]. Further work is currently being done to verify that the background model used by SimCADO is able to also reliably

[11] https://www.eso.org/sci/observing/phase2/ObsConditions.html

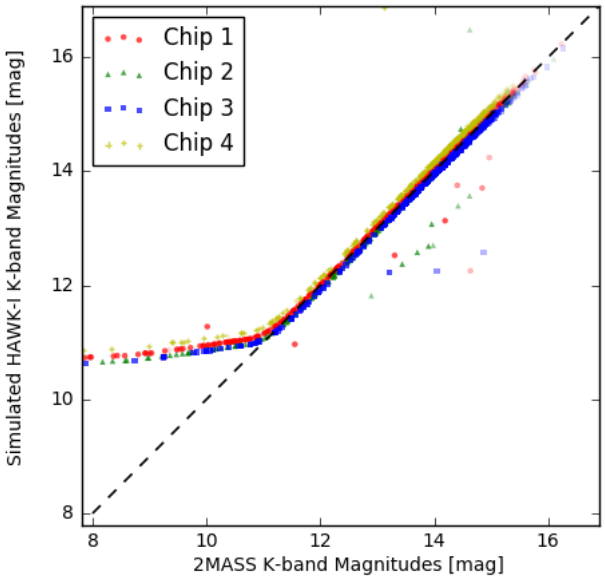

Fig. 5. Instrumental K-band magnitudes from image of M4 simulated with SimCADO versus the 2MASS catalogue K-band magnitude. The zero-point used was 27.2^m. The one-to-one correlation was to be expected because the description of M4 used by SimCADO to generate the images was based on the 2MASS catalogue. The deviations from the one-to-one line show where the photometry pipeline we used broke down. The cloud of points below the line show were two stars were close enough together that the pipeline chose the wrong star. It was set up to choose the brightest star within a 1" radius each set of coordinates. Secondly the deviation from the one-to-one line around Ks=$11^m$is due to the fixed aperture used in the photometry pipeline. The wings of the HAWK-I PSF meant that the flux from stars brighter than Ks=11^mleaked into the background aperture. Consequently an incorrectly high background flux was subtracted from the star, artificially lowering its measured magnitude. The effect of the different gain values for the HAWK-I detector chips is also visible as the slight offset between the different coloured dots.

reproduce the sky background for other combinations of observing conditions such as airmass, seeing and precipitatable water vapour. The results of this study will also be reported in the companion paper.

5. Predictions for MICADO's point source sensitivity

MICADO will offer diffraction limited imaging with a PSF width of ~7 and ~12 milli-arcseconds in the J and Ks filters respectively. This will allow stars in densely populated regions such as the centres of open and globular clusters to be easily resolved (See Figure 6.2). Indeed the majority of the primary science cases for MICADO revolve around resolving stellar populations or astrometry of objects in very dense regions (e.g. the galactic centre). Thus it is important to know the sensitivity limits of the imaging mode well in advance of MICADO going on-sky. Here we briefly present the results of a series of SimCADO simulations aimed at determining the observational limits for MICADO. The model of the optical train used for these simulations was the default MICADO wide-field imaging mode, as described in section 2. The method for measuring the signal to noise ratio was identical to the method used for the HAWK-I verification run described in section 4, except the minimum integration time was extended to 2.6 seconds to reflect the read out time of the HAWAII-4RG detectors that have been ear-marked for MICADO. Also the grid of stars used for the test observations included only stars with magnitudes between 16 and 32 as the extended diffraction spikes from brighter stars negatively affected the photometry of the nearby fainter stars. The extent to which such PSF artefacts influence the accuracy both the photometry as well as the completeness of observed stellar populations is indeed an important question and will be addressed in a companion paper. For this study however we simply removed the stars whose PSF artefacts were contaminating their neighbours aperture.

!!! Get fabrice to write a paragraph on this? !!!

It should be noted that the PSFs for these simulations were produced by the SCAO working group as part of the MICADO consortium (Vidal et al., 2017) specifically for inclusion in the SimCADO package. They were generated using the current state-of-the-art adaptive optics simulations and describe the residual PSF after the AO loop has been closed. The simulations were run for a 14.7^mguide star that is 5" off-axis. The targets were observed at the zenith. The Strehl Ratio of the PSFs were 0.29, 0.51 and 0.68 for the J, H and Ks band respectively.

5.1. Point source sensitivity vs exposure time

For studies of stellar populations, the detection limit is often set to 5σ, where $\sigma$is the level of background noise in an image. However in order to achieve a high level of astrometric precision (e.g. down to levels of ~1/30th of a pixel, or ~50muas), a much higher signal to noise ratio is required, e.g. ~250σ. Table 4 lists MICADOs limiting magnitudes for the photometric ($5\sigma$and 10σ) and astrometric cases. For an exposure time of 5 hours, we find the limiting magnitudes (Vega) for a 5σdetection to be 28.7^m, $27.9^m$and 27.3^min the J, H and Ks broadband filters respectively. For the narrowband filter Brγwe find a limiting magnitude of 26.0^m. The J and H limiting magnitudes match those from the ELT exposure time calculator[12] to $<0.1^m$. The Ks estimate is 0.2^mweaker than that for the ETC.

For astrometric purposes (~250σ), we find the required magnitudes to be 24.2^m, 23.5^m, 22.9^min J, H and Ks filters and 21.7^min the Brγfilter. All magnitudes here all listed in the Vega system.[13] Figure 5.1 is an expanded graphical representation of table 4 that shows the full range of limiting magnitudes for observations from the shortest integration time to a full 10 hour observing program and for signal to noise ratios of $1\sigma$to 1000σ(i.e. no detection to saturated star).

5.2. Point source saturation limits

Given the ELT's collecting area of ~978m^2, it is also important when determining observational strategies to know the saturation limits of the detectors. Basic aperture photometry is only reliable when the maximum pixel values inside the aperture are below the saturation threshold. Advanced techniques such as PSF fitting will naturally allow this threshold to be extended, however given the unorthodox shape, the many relatively sharp artefacts, and the dynamic nature of an AO corrected PSF, the use of advanced photometric methods will prove challenging. Therefore in order to set (conservative) limits on the accuracy of photometry for bright sources with MICADO we decided to define photometric reliability as stars with only unsaturated pixels. When

[12] `https://www.eso.org/observing/etc/bin/simu/elt_ima`
[13] To convert to the AB system ~0.9, ~1.4 and ~1.85 should be added to the J, H and Ks magnitudes respectively.

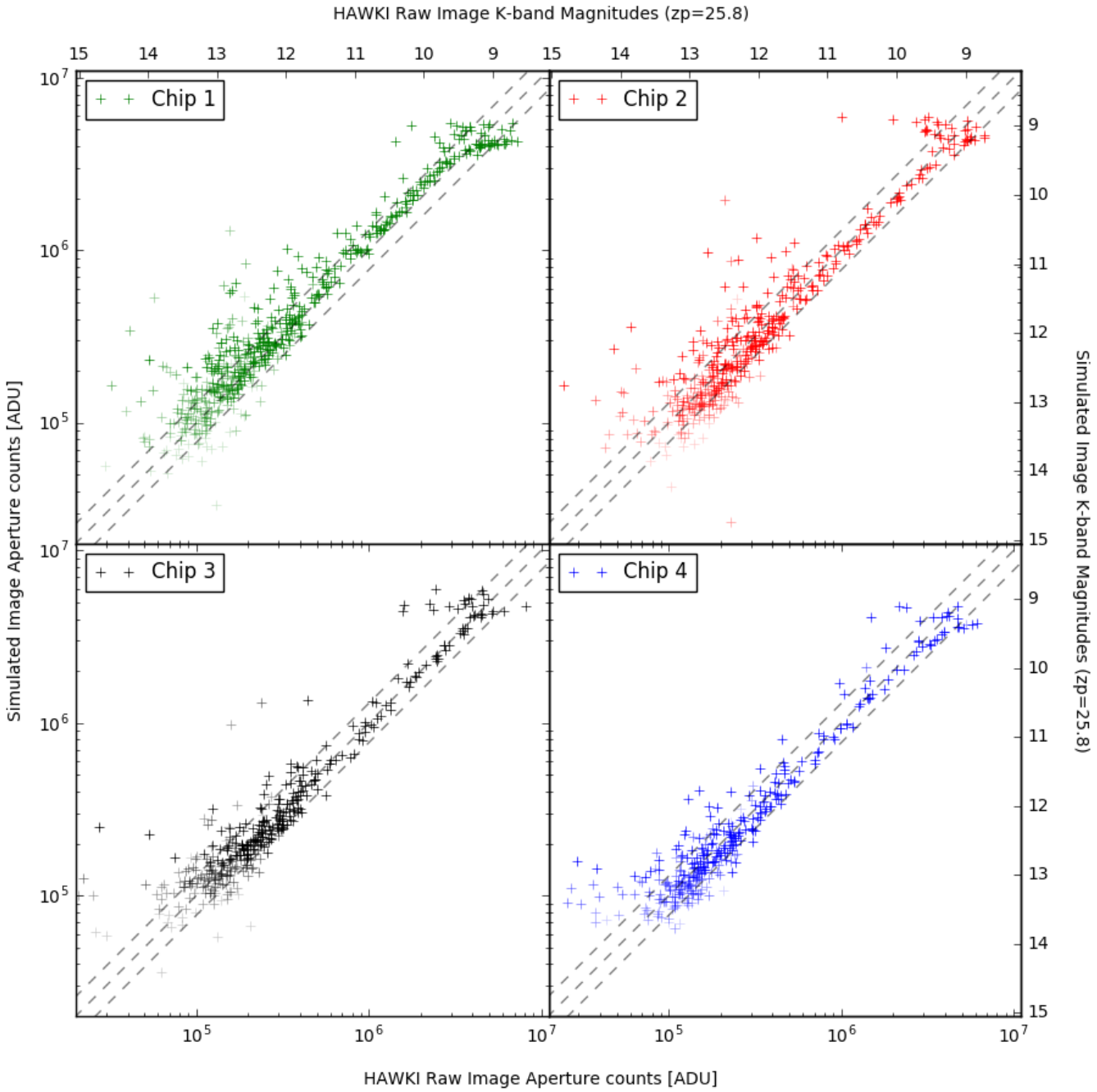

Fig. 6. Flux counts from aperture photometry of the stars in the simulated and real Ks-band images of M4. Each of the detector chips is plotted here as they each covered a different region of M4 and each chip has a different gain factor. The strength of the symbols is determined by the photometric quality flag in the 2MASS catalogue. The dashed lines are the $\pm 0.3^m$, or 30% flux difference intervals. For each chips 1 and 2 >75% of stars with A-grade 2MASS photometry fall within these bands. For chips 3 and 4 this figure is >85%. ~55% of the sources with C-grade or less photometry flags fell outside the ±30% bands. When investigating these sources we found a large fraction to be single entries in the 2MASS catalogue which were resolved out into two stars in the HAWK-I images.

reading Figure 5.1 saturation begins to occurs roughly in the regime of SNR>750.

The minimum read-out time for a full H4RG detector will be ~2.6 seconds. MICADO will also over a fast readout mode for a windowed region of the detector capable of reading out a 100x100 pixel area at a rate of 200 Hz (DIT ~5ms). To calculate the bright star limits we took the brightest star from the simulated images which had no values over the correctable non-linear regime. As there is little data publicly available for the performance of HAWAII-4RG detectors, we assumed the characteristics will be similar to the HAWAII-2RG chips. According to Loose et al. (2007) all detectors in the HAWAII-RG family have a correctable linearity regime (within 5%) of ~10^5 e-/pixel with a full well depth of <1.5×10^5 e-/pixel. Table 5 shows the

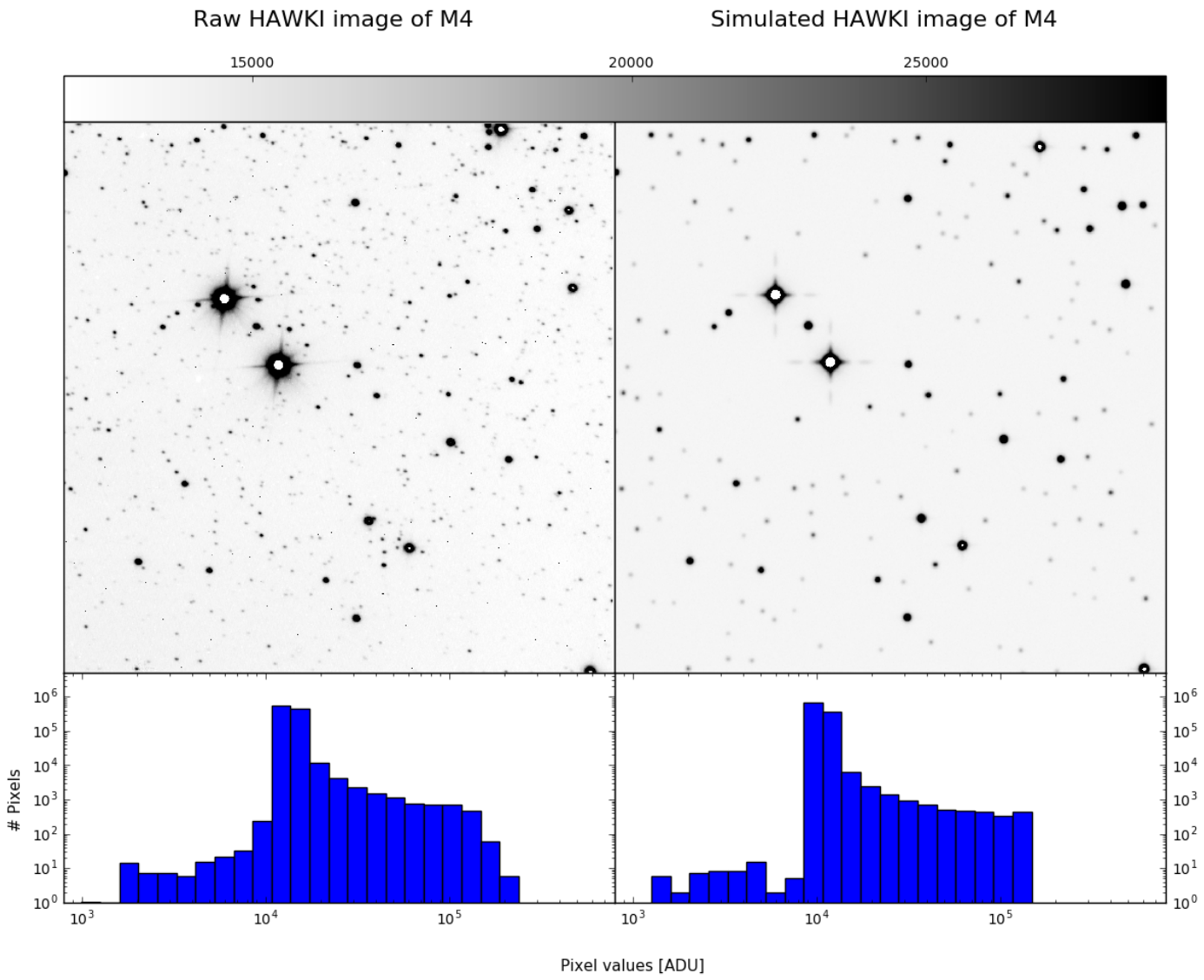

Fig. 7. Top: A comparison of a raw HAWK-I image with a simulated image from SimCADO for the same field near M4. Features created by the optical train (e.g. diffraction spikes) and by the detector (e.g. saturation) can be seen in both the real and simulated images. The width of the PSF in the simulated images is smaller than in the real images because SimCADO does not currently model leakage from saturated pixels into neighbouring pixels. The background flux in the simulated image is $\sim 0.3^m$/arcsec^{2}lower than in the real image due to worse than average atmospheric conditions during the observation. Bottom: The distribution of pixel counts for the real (left) and simulated (right) images is given here to illustrate that SimCADO is capable of recreating observations with no "real world" input. The simulated image was built up step by step from data files containing information for individual effects present in the HAWK-I+UT4 optical train.

brightest magnitudes that can be observed in the J, H, Ks and Brγfilters without any pixels saturating. As a sanity check, we compared 5 to the saturation limit given by the ELT exposure time calculator. The ETC uses a slightly different configuration for the imaging mode. The most notable differences being a collecting area of 1100 m^2 and a plate scale of 5 mas. After normalising the results from the ETC, we find that SimCADO matches the ETC's calculations to within 0.1^m.

It is worth noting that in the standard wide-field imaging mode with an integration time of 2.6 seconds, MICADO will saturate at the sensitivity limit of the 2MASS survey (J=15.8^m, H=$15.1^m$and Ks=14.3^mSkrutskie et al. (2006)). On the one hand this is a testament to the extreme increase in observing capabilities that the ELT and MICADO will provide. On the other hand this will prove problematic for observers as all observations within ∼1' of a 2MASS source will need to account for the effects of overly bright sources. Given that the diffraction spikes of the ELT's PSF are long and prominent, there is a good chance that they will cause issues with the reduction and analysis of fainter, more interesting regions.

5.2.1. Extended Source sensitivities

With the ELT's 978 m^2 collecting area and the diffraction limited performance afforded by both MCAO and SCAO modes, MICADO will have an unprecedented ability to observe faint point sources. Extended sources will however not see the same level of improvement. To a good approximation, the flux per resolution element from a point source scales linearly with collecting area, irrespective of the size of the resolution element. For extended

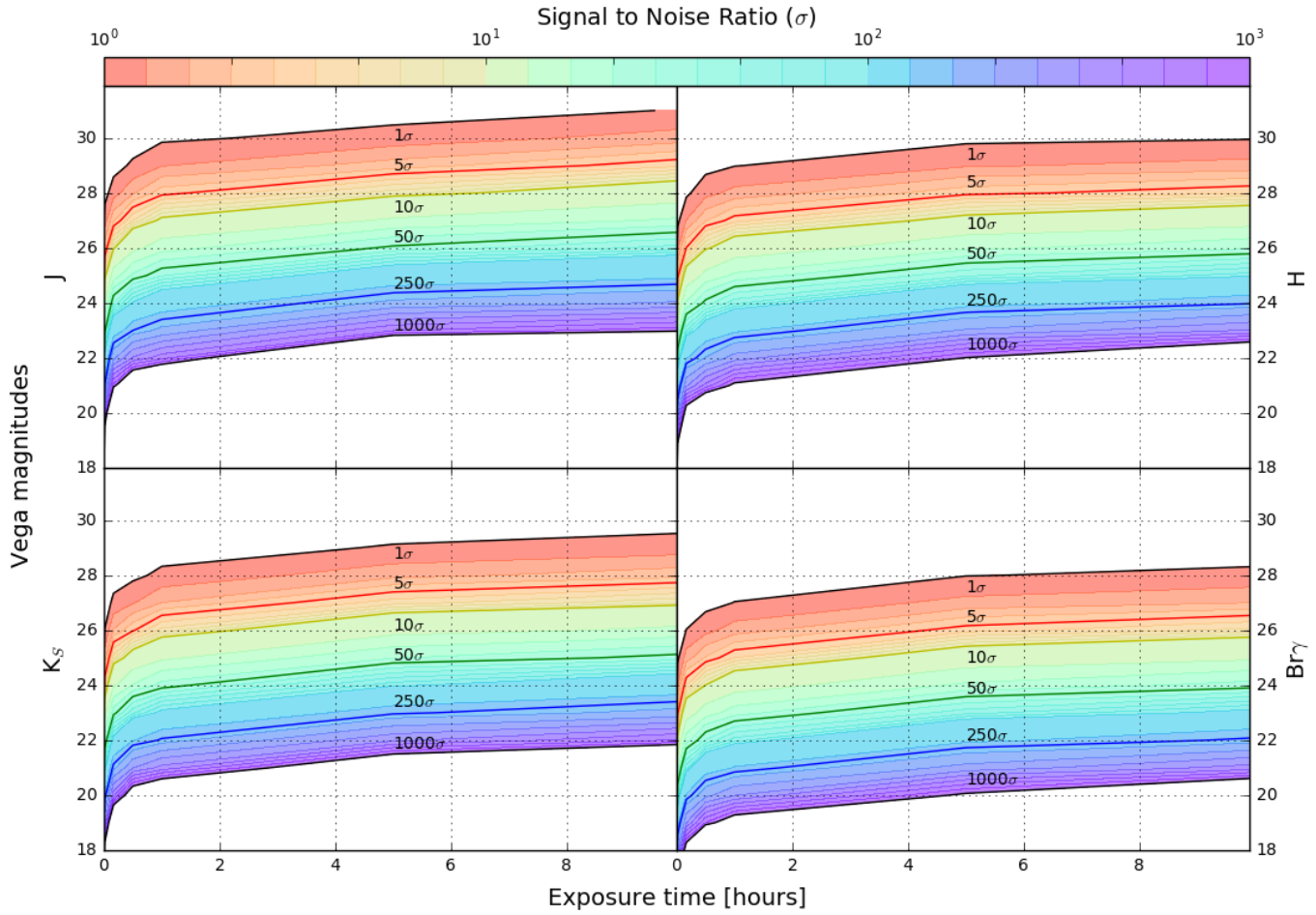

Fig. 8. Limiting magnitude plots for the wide field (4mas per pixel) imaging mode of MICADO at the ELT in Vega magnitudes. Signal to noise ratios above 5$\sigma$are sufficient for photometry. High precision astrometry requires stronger detections ~250σ. Saturation of pixels for point sources begins around >750σ. It should be noted that these magnitudes apply to the current design of MICADO and the ELT. At the time of publication MICADO is still in its preliminary design phase. As such we expect small changes in these values as the MICADO design matures.

sources however, flux scales inversely with the angular area of the resolution element. This can be expressed as:

For point sources: $F \propto F_0 \times A$

For extended sources: $F \propto F_0 \times A \times p^2$

where F_0 is the normalised incoming flux, A is the collecting area of the telescope, and p is the plate scale of the detectors. A quick comparison with the values of the NIR arm of the WFC3 instrument **??** on the Hubble Space Telescope (HST) shows that MICADO will be a factor of almost five times less efficient than the WFC3-IR instrument when it comes to collecting light from extended sources. However MICADO will provide a vast improvement in our ability to resolve structures on scales ~32× smaller than WFC3-IR on HST. For example at a redshift of $z = 2$ where the proper angular transverse distance is at it's smallest (~8.5 kpc/arcsec), MICADO should be able to resolve structures on scales of ~30 pc. This is compared to scales of 300 pc and 1 kpc with JWST and HST respectively.

Will we do a more detailed investigation for extended sources here ???

List background fluxes for each filter and work backwards to get the 5σsensitivity for a given exposure time - easy right?

5.3. Spectral type with distance

Four of the major science drivers for MICADO rely on determining the properties of stellar populations. Hence we found it prudent to use the sensitivity estimates from SimCADO to calculate limiting distances for a 5σdetection for different spectral types. Figure 5.3 shows the apparent magnitude of a selection of main sequence stars with increasing distance as well as the sensitivity limits for MICADO for a range of exposure times. We used the main sequence absolute magnitudes given in Table 5 of Pecaut & Mamajek (2013)[14]. As the brightest stars in the main sequence cover almost the same magnitude range as all giant and most supergiant stars, those readers interested in the limiting distances for stars which have left the main sequence are requested to use the distances for a main sequence star with an equivalent absolute magnitude. Using SimCADO we have determined that MICADO should be able to detect all A-type stars in Centaurus A at a distance of 4 Mpc with a 5 hour observation. A 1 hour observation should be sufficient to detect all stars

[14] Additional information for the L and T dwarves (not reported in (Pecaut & Mamajek 2013)) were taken from the associated website `http://www.pas.rochester.edu/~emamajek/EEM_dwarf_UBVIJHK_colors_Teff.txt`

Filter	SNR	2.6 sec	10 sec	1 min	10 min	1 hr	5 hrs	10 hrs
	5σ	23.4^m	24.4^m	25.6^m	26.7^m	27.8^m	28.7^m	29.0^m
J	10σ	22.6^m	23.6^m	24.8^m	26.0^m	27.0^m	27.9^m	28.2^m
	250σ	18.7^m	19.9^m	21.1^m	22.4^m	23.4^m	24.2^m	24.6^m
	5σ	23.0^m	23.8^m	24.8^m	26.0^m	27.0^m	27.9^m	28.3^m
H	10σ	22.2^m	23.0^m	24.0^m	25.3^m	26.2^m	27.1^m	27.5^m
	250σ	18.6^m	19.4^m	20.4^m	21.7^m	22.7^m	23.5^m	23.9^m
	5σ	22.4^m	23.1^m	24.1^m	25.6^m	26.4^m	27.3^m	27.7^m
Ks	10σ	21.6^m	22.4^m	23.4^m	24.8^m	25.6^m	26.5^m	26.9^m
	250σ	18.0^m	18.9^m	19.8^m	21.0^m	22.1^m	22.9^m	23.3^m
	5σ	20.6^m	21.8^m	22.9^m	24.1^m	25.2^m	26.0^m	26.3^m
Brγ	10σ	19.8^m	21.0^m	22.1^m	23.4^m	24.4^m	25.2^m	25.6^m
	250σ	16.0^m	17.1^m	18.4^m	19.8^m	20.8^m	21.7^m	22.1^m

Table 4. Specific point source sensitivities for the NIR broadband filters J, H and Ks and the narrow band filter Brγ. $5\sigma$and $10\sigma$are generally accepted detection limits for photometric measurements, while for accurate astrometry signal to noise ratios above $250\sigma$are required. The errors on these magnitudes is $\pm 0.1^m$. It should be noted that these magnitudes apply to the current design of MICADO and the ELT. At the time of publication MICADO is still in its preliminary design phase. As such we expect small changes in these values as the MICADO design matures.

Filter	DIT	4mas pixel	1.5mas pixel
J	2.6s	15.9^m	13.6^m
	0.005s	14.0^m	11.8^m
H	2.6s	15.6^m	13.4^m
	0.005s	13.8^m	11.6^m
K_S	2.6s	14.8^m	12.5^m
	0.005s	13.0^m	10.8^m
Brγ	2.6s	12.0^m	9.9^m
	0.005s	10.2^m	8.1^m

Table 5. Saturation Limits for MICADO assuming a effective detector well depth of 10^5 e-/pixel. The shortest integration time for a full detector will be ~2.6s, while a faster readout mode will be available for smaller windowed regions (Davies et al. 2010). Given the current detector specifications a 100×100 pixel window might achieve a readout frequency of 200 Hz, or 5ms per exposure. The limits are split between the two default imaging modes of MICADO: Wide-field mode (4mas/pixel, ~50" FoV), and the zoom mode (1.5mas/pixel, ~20" field of view). While the ESO exposure time calculator for the ELT has a slightly different configuration for the imaging mode, when the results are normalised we find that the SimCADO saturation limits are within $0.1^m$of the ETC's limits.

down to the Hydrogen burning limit (M >0.08 M$\odot$) in the Magellanic Clouds (50 kpc). However it is worth mentioning that at this distance all stars brighter than B1V will saturate within the shortest exposure time (DIT = 2.6 sec). For more case specific distance limits based on the SimCADO limiting magnitudes, we direct the reader to Figure 5.3. The equivalent plot for the Ks band is included in the Appendix. These distance estimates are based on an ideal case scenario and the current design of the MICADO optical train. Therefore Figure 5.3 should be understood as illustrating upper limits for the distance estimates. For example, we have assumed no extinction along the line of sight. Nor have we taken into account the increased background levels in crowded field. Both effects will undoubtedly reduce the distance estimated by varying amounts. To what degree the level of crowding affects these distance estimates will be the focus of a companion paper.

6. Discussion, open issues and assumptions

6.1. Discussion on the differences between the simulated and the real HAWK-I images

Overall the simulated images of M4 and NGC4147 compared favourably with the raw observations from the ESO archive. The main image characteristics, such as the distribution of pixel flux, background level and noise, total star fluxes and positions, detector noise and saturation, were well reproduced in the simulated images. Magnitudes derived from aperture photometry on the simulated images matched almost perfectly with the 2MASS catalogue for all stars with J/Ks>11^m. When comparing photometry between the simulated and archive images, around two thirds of all the stars measured had flux differences between the images of <0.3^m. The scatter seen in Figure 4.3 is an product of aperture photometry on a real, but unprocessed HAWK-I image, and not due errors in SimCADO's treatment of stellar fluxes. Because the HAWK-I images were based on the 2MASS catalogue, contamination from sources fainter than the catalogue detection limit were not included in the simulated images. Hence this scatter shows that there is still room for improvement when it comes to SimCADO simulating the true sky background for an image. With the ELT's ability to detect sources down to J≈29^m, the prevalence of background sources in this regime will indeed need to be addressed and simulated accurately.

The level of background flux generated by SimCADO for the J and Ks filters is in line with the flux levels returned by the ESO exposure time calculator for HAWK-I. However only half of the J and Ks images from the archive had background levels as low as the ETC and SimCADO. The other two J and Ks images had levels 10% and 30% higher. While there is an abundance of information on the weather conditions during the observations, we were unable to find estimates for the measured sky background. We therefore used the standard Paranal background magnitudes for the simulations. As NIR sky background levels can vary up to 0.75^mover the course of a night (Moreels et al. 2008b), we don't see the difference between the simulated and real background fluxes in these images as a major failure of the software. Moreover it is yet another effect which should be added to a future release of SimCADO.

A final caveat for the software verification is that the model of the optical train for UT4/HAWK-I is based on the information available on the ESO website and from the HAWK-I user manual. Despite our due diligence it is possible that some of the data

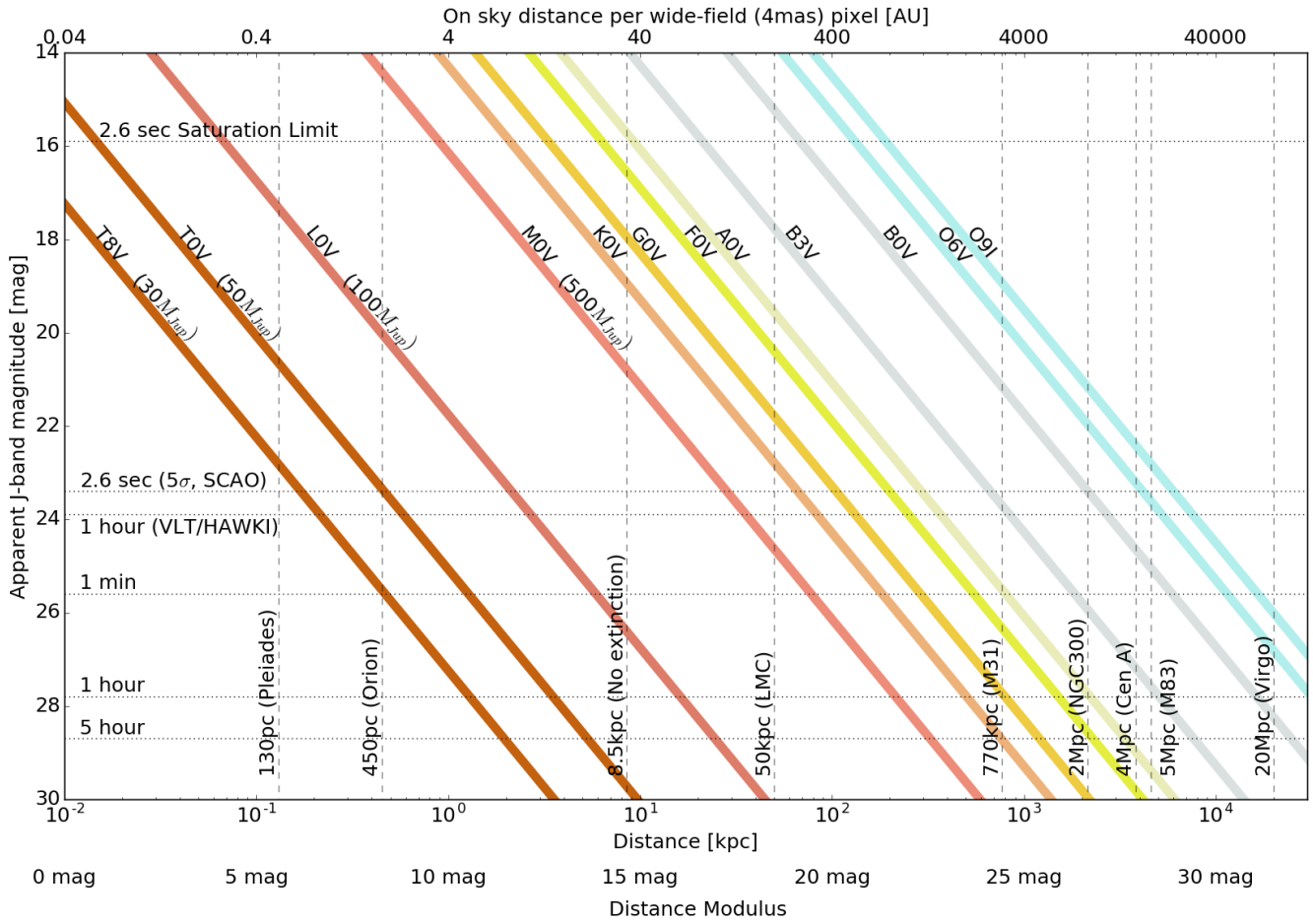

Fig. 9. The colourful lines represent the apparent magnitude of the major spectral types with increasing distance. The dashed horizontal lines, unless otherwise stated, represent the 5σ detection limits for various exposure times with MICADO. When a coloured line crosses below a horizontal line, it means that this type of main sequence star will no longer be detectable by MICADO at the distance when the cross occurs. As a reference the dashed vertical lines show distances to well known astronomical objects. It is worth noting that what HAWK-I can do in 1 hour, MICADO can do in 2.6 seconds. While this comparison may seem ludicrous, the ELT has a primary mirror ~20× larger that of UT4 at the VLT and the smaller plate scale of MICADO means a factor of ~35× less background flux per pixel.

used by SimCADO is inaccurate or not up to date. In order to further test the how SimCADO reacts to different sets of observing conditions (Airmass, Seeing, etc), we submitted a ESO proposal in Period 100 for technical time on HAWK-I. We are waiting on the completion of the observing run before embarking on a new validation campaign.

6.2. Accuracy of the SimCADO sensitivity predictions

SimCADO was verified by comparing simulated images with real HAWK-I observation. Furthermore estimates from SimCADO images of the detection and saturation limits for observations with MICADO fall within $0.1^m$of the values given by the ELT exposure time calculator (after normalising the two optical train configurations). These two results give us confidence that the predictions of MICADOs sensitivity can be accurately determined from simulations with SimCADO. These simulation have however been conducted using several simplifications. For example, the atmospheric conditions were assumed to mirror those of the average night at Paranal. Given that the NIR sky background can vary up to ~0.2^mwithin 15 minutes (Moreels et al. 2008b) and is also dependent on the level of water in the air as well as the airmass of the pointing, it is clear that the true detection limits of MICADO will vary from the SimCADO predictions. Furthermore the PSF used for the current round of SimCADO predictions was uniform across the field of view. This will definitely not be the case. Reductions in the Strehl Ratio of >50% over the MICADO field of view are expected for SCAO observation (Clénet et al. 2015). Such variations will have a marked impact on sensitivity in the outer regions of the MICADO focal plane.

Aside for estimating the performance of the telescope and instrument are, by far the biggest challenge will be the ELT's PSF. Accurate photometry of bright sources, extracting faint sources that are covered by the wings of the brighter sources, and accurate astrometry all depend on the accurately knowing the shape of the PSF. As can be seen in Figure 6.2, the discrete nature of the diffraction spikes of the SCAO PSF could easily confuse a star finding algorithm. Additionally the PSF will rotate with respect to the field over the course of an observing run due to the ELT's alt-azimuth mount. This would greatly complicate the standard stack and subtract technique for data reduction. Arguably though, this may prove advantageous as it would

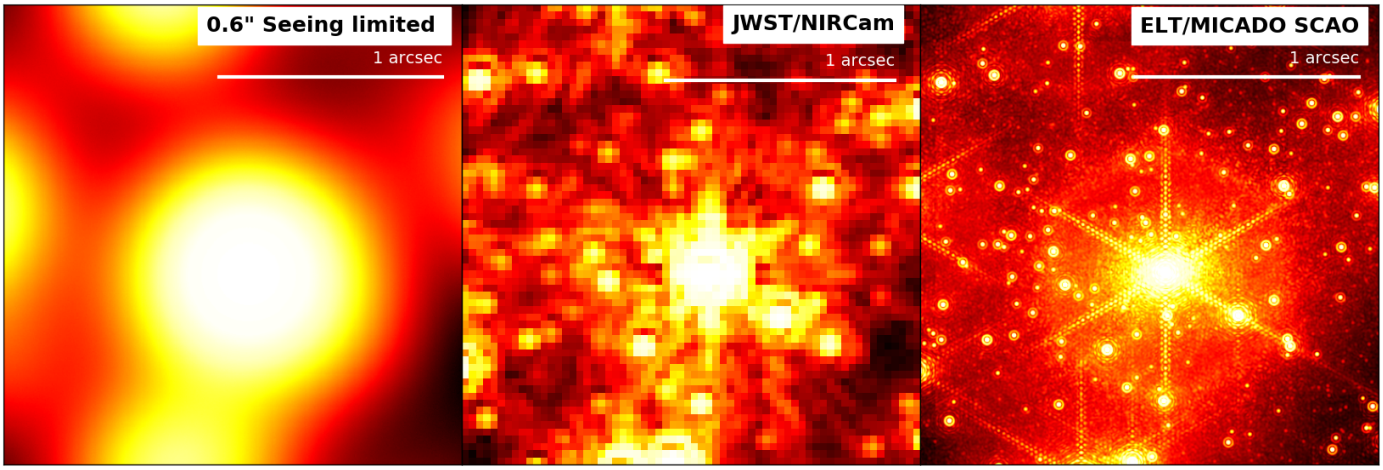

Fig. 10. An illustration of the improvement that MICADO's increase in resolution will bring to the field of stellar populations. Left: A dense stellar field observed with 0.6 arcsecond Seeing. Middle: The same field as will be observed by NIRCam on JWST. Right: A prediction of how the dense stellar field will look when observed by MICADO in wide field mode (4 mas/pixel).

allow rotational dithering to smooth out the sharp features of the PSF. An alternative approach would be to deconvolve the images with a spatially varying model of the PSF. This would however require multiple descriptions of the PSF for each detector frame, which could slowly become a challenging data management task. Whether this task then belongs in the automated data pipeline or is left to the user is still undecided. A different approach would be to use a blind deconvolution algorithm (Vorontsov & Jefferies 2017). Recent results are encouraging however it remains to be seen whether how well this approach works for spatially varying PSFs.

In any case the complex PSF of the ELT will present a challenge to standard data analysis techniques. How the PSF artefacts of bright stars affect the surrounding environment is a question which should be addressed when still in the early stages of planning observations with the ELT and MICADO. Ideally this should already be considered during the proposal phase. This gives us the justification to further develop tools like SimCADO so that observers can visualise in advance the impact that a segmented mirror will have on diffraction limited observations.

6.3. Future functionality for SimCADO

Although the results of the first verification run show, SimCADO is capable of recreating observations with only descriptions of the optical elements as input. The simulated image was built up step by step from data files containing information for individual effects present in the UT4/HAWK-I optical train. There are however still several aspects that require attention by the development team - each of which will be addressed in detail in a companion paper. In short they are:

Atmospheric variations: SimCADO uses a standardised spectrum for the sky background, which is scaled to the required background level to provide the background flux for any chosen filter. Currently this atmospheric spectrum is independent of the observational setup, i.e. it does not change as Airmass or PWV conditions change. For the verification run described here, these points weren't relevant: the archival data for M4 were taken close to Zenith and the image of NGC4147 (Airmass ~1.44) was primarily used as a control for its different exposure length. Functionality to accurately model the effects of different observational conditions are in development and will be included in a future release of the software.

PSF variability: While not as important for a Seeing limited instrument such as HAWK-I (before the recent GRAAL upgrade) the varying shape of the PSF over the field of view in observations conducted with adaptive-optics is not a trivial effect. The development team is currently in the process of implementing functionality to include the off-axis PSFs provided by the SCAO and MCAO simulation teams. Furthermore the PSF is based on the post-AO PSF delivered by the AO simulation teams. The exposure times are assumed to be long enough that the PSF shouldn't vary noticeably between exposures. Whether or not this assumption holds for all time scales remains to be investigated.

Distortion effects: For photometric studies optical distortions are a nuisance. However for astrometric studies they are absolutely critical. SimCADO includes the functionality to shift point sources on the sub-pixel level. As such we are currently investigating the best way to implement the use of distortion maps.

Spectroscopy: MICADO will also include the optics to function as a long slit spectrograph. Development is ongoing with the implementation of this mode into SimCADO.

Non-common path aberrations: Only the effective loss in flux due to NCPAs is currently included in SimCADO. This is a function of wavelength and as such can be modelled effectively as an additional transmission curve. The spatial aspects of the NCPAs in the context of the MICADO optical train need to be investigated further before we can implement them into SimCADO.

Although there is still much work to do, SimCADO is already capable of simulating raw detector read-outs for each of the MICADO imaging modes. This alone covers the majority of the primary science drivers for MICADO. It should also be noted that MICADO is still in the initial design phase and so the composition of the optical train, and therefore the default data installed alongside SimCADO, are likely to change in the future. However we foresee no radical changes to the design, and thus no radical changes to the sensitivity estimates we have presented in this paper.

7. Summary

As part of the design activities for the MICADO instrument we have developed an instrument data simulator in Python: SimCADO. The software is capable of generating detector frames for any given optical train configuration and source object description. A summary of our activities and results is as follows:

- In conjunction with the MICADO instrument team we have developed a modular python package which allows us to model each element in the optical train separately. The software allows the user to fully control the configuration of the optical train as well as the description of the astronomical object to be observed. Images produced by the package are in the standard FITS format and can be treated as coming directly from a telescope.
- We configured SimCADO to mimic the UT4/HAWK-I optical train and "observed" two globular clusters with this setup. A comparison to archive data for the same globular clusters showed that SimCADO is capable of reproducing all the major and most of the minor effects that are seen in raw detector frames from HAWK-I. A photometric comparison showed a one-to-one correlation between the flux observed in the archive and simulated images. Although there was scatter around this line, the primary source of uncertainty lay with the photometric analysis of the archive data and not with the simulated images. Additionally SimCADO was able to reproduce the detection limits given by the ESO exposure time calculator for a 1-hour observation with HAWK-I.
- Using the configuration for the ELT/MICADO optical train we simulated a grid of stars to find the detection limits for different exposure times. We have shown that the 5 hour detection limits in Vega magnitudes are: J=28.7^m, H=27.9^{m}and Ks=27.3^m, while the saturation limit for the shortest exposure time (MINDIT=2.6 s) in the wide-field (4 mas/pixel) mode are similar to the 2MASS detection limit: J=15.9^m, H=15.6^{m}and Ks=14.8^m. The use of the zoom mode (1.5 mas/pixel) in conjunction with a narrow band filter would reduce increase this limit to Brγ=9.9^m.
- With these detection limits we have shown that MICADO will be capable of detecting individual A0 V stars at a distance of 4 Mpc (Centaurus A), while any star brighter than B1 V at a distance of 50 kpc (LMC) will saturate during the a single read-out time.
- We will be adding the following functionality in the near future: a long slit spectrographic mode, field variable PSFs, variations in atmospheric conditions, as well as further support for the high time resolution and astrometric imaging modes.

We encourage anyone who may want to use the ELT and MICADO for future observations to simulate their science case in advance. Not only will this help astronomers to get a feel for what MICADO will be capable of and where possible problems with an observing strategy will be, it will also help developing the software further to meet the needs of the astronomical community.

Acknowledgements. SimCADO incorporates Bernhard Rauscher's HxRG Noise Generator package for pythonRauscher (2015). This research made use of POPPY, an open-source optical propagation Python package originally developed for the James Webb Space Telescope project Perrin et al. (2015). This research made use of Astropy, a community-developed core Python package for Astronomy (Astropy Collaboration et al. 2013; The Astropy Collaboration et al. 2018). This research made use of Photutils (Bradley et al. 2017). This research has made use of "Aladin sky atlas" developed at CDS, Strasbourg Observatory, France (Bonnarel et al. 2000; Boch & Fernique 2014). SimCADO makes use of atmospheric transmission and emission curves generated by ESO's SkyCalc service, which was developed at the University of Innsbruck as part of an Austrian in-kind contribution to ESO. Based on data obtained from the ESO Science Archive Facility under request number Leschinski, #331857 This publication makes use of data products from the Two Micron All Sky Survey, which is a joint project of the University of Massachusetts and the Infrared Processing and Analysis Center/California Institute of Technology, funded by the National Aeronautics and Space Administration and the National Science Foundation (Skrutskie et al. 2006). This research is partially funded by the project IS538003 of the Hochschulraumstrukturmittel (HRSM) provided by the Austrian Government and administered by the University of Vienna. The authors would also like to thank all the members of the consortium for their effort in the MICADO project, and their contributions to the development of this tool. KL would like to thank the following people for their patience and support of the past three years: João Alves, Michael Mach, Oliver Czoske, Rainer Köhler, Stefan Meingast, Werner Zeilinger and Wolfgang Kausch. KL would also like to express his gratitude to Eline Tolstoy, Gijs Verdoes Kleijn and Richard Davies for their many insightful and helpful discussions regarding the development of MICADO.

References

Astropy Collaboration, Robitaille, T. P., Tollerud, E. J., et al. 2013, A&A, 558, A33
Boccas, M., Vucina, T., Araya, C., Vera, E., & Ahhee, C. 2006, Thin Solid Films, 502, 275
Boch, T. & Fernique, P. 2014, in Astronomical Society of the Pacific Conference Series, Vol. 485, Astronomical Data Analysis Software and Systems XXIII, ed. N. Manset & P. Forshay, 277
Bonnarel, F., Fernique, P., Bienaymé, O., et al. 2000, A&AS, 143, 33
Bradley, L., Sipocz, B., Robitaille, T., et al. 2017, astropy/photutils: v0.4
Brandl, B. R., Lenzen, R., Pantin, E., et al. 2008, in Proc. SPIE, Vol. 7014, Ground-based and Airborne Instrumentation for Astronomy II, 70141N
Clénet, Y., Buey, T., Rousset, G., et al. 2016, in Proc. SPIE, Vol. 9909, Society of Photo-Optical Instrumentation Engineers (SPIE) Conference Series, 99090A
Clénet, Y., Gendron, E., Gratadour, D., Rousset, G., & Vidal, F. 2015, A&A, 583, A102
Cuby, J. G., Lidman, C., & Moutou, C. 2000, The Messenger, 101, 2
Davies, R., Ageorges, N., Barl, L., et al. 2010, in Proc. SPIE, Vol. 7735, Ground-based and Airborne Instrumentation for Astronomy III, 77352A
Davies, R., Schubert, J., Hartl, M., et al. 2016, in Proc. SPIE, Vol. 9908, Society of Photo-Optical Instrumentation Engineers (SPIE) Conference Series, 99081Z
Dierickx, P., Enard, D., Merkle, F., Noethe, L., & Wilson, R. N. 1990, in Proc. SPIE, Vol. 1236, Advanced Technology Optical Telescopes IV, ed. L. D. Barr, 138–151
Diolaiti, E. 2010, The Messenger, 140, 28
Diolaiti, E., Ciliegi, P., Abicca, R., et al. 2016, in Proc. SPIE, Vol. 9909, Society of Photo-Optical Instrumentation Engineers (SPIE) Conference Series, 99092D
Finger, G., Dorn, R. J., Eschbaumer, S., et al. 2008, in Proc. SPIE, Vol. 7021, High Energy, Optical, and Infrared Detectors for Astronomy III, 70210P
Gilmozzi, R. & Spyromilio, J. 2007, The Messenger, 127
Jones, A., Noll, S., Kausch, W., Szyszka, C., & Kimeswenger, S. 2013, A&A, 560, A91
Kissler-Patig, M., Pirard, J.-F., Casali, M., et al. 2008, A&A, 491, 941
Leschinski, K., Czoske, O., Köhler, R., et al. 2016, in Proc. SPIE, Vol. 9911, Society of Photo-Optical Instrumentation Engineers (SPIE) Conference Series, 991124
Loose, M., Beletic, J., Garnett, J., & Xu, M. 2007, in Proc. SPIE, Vol. 6690, Focal Plane Arrays for Space Telescopes III, 66900C
Moreels, G., Clairemidi, J., Faivre, M., et al. 2008a, Experimental Astronomy, 22, 87
Moreels, G., Clairemidi, J., Faivre, M., et al. 2008b, Experimental Astronomy, 22, 87
Noll, S., Kausch, W., Barden, M., et al. 2012, A&A, 543, A92
Pecaut, M. J. & Mamajek, E. E. 2013, ApJS, 208, 9
Perrin, M. D., Long, J., Sivaramakrishnan, A., et al. 2015, WebbPSF: James Webb Space Telescope PSF Simulation Tool, Astrophysics Source Code Library
Peterson, J. R., Jernigan, J. G., Kahn, S. M., et al. 2015, ApJS, 218, 14
Posselt, W., Holota, W., Kulinyak, E., et al. 2004, in Proc. SPIE, Vol. 5487, Optical, Infrared, and Millimeter Space Telescopes, ed. J. C. Mather, 688–697
Rauscher, B. J. 2015, PASP, 127, 1144
Schmalzl, E., Meisner, J., Venema, L., et al. 2012, in Proc. SPIE, Vol. 8449, Modeling, Systems Engineering, and Project Management for Astronomy V, 84491P

Skrutskie, M. F., Cutri, R. M., Stiening, R., et al. 2006, AJ, 131, 1163
Stone, R. C. 1996, PASP, 108, 1051
Thatte, N., Tecza, M., Clarke, F., et al. 2010, in Proc. SPIE, Vol. 7735, Ground-based and Airborne Instrumentation for Astronomy III, 77352I
The Astropy Collaboration, Price-Whelan, A. M., Sipőcz, B. M., et al. 2018, ArXiv e-prints [arXiv:1801.02634]
Vorontsov, S. V. & Jefferies, S. M. 2017, Inverse Problems, 33, 055004
Winkler, R., Haynes, D. M., Bellido-Tirado, O., Xu, W., & Haynes, R. 2014, in Proc. SPIE, Vol. 9150, Modeling, Systems Engineering, and Project Management for Astronomy VI, 91500T
Wright, S. A., Walth, G., Do, T., et al. 2016, in Proc. SPIE, Vol. 9909, Society of Photo-Optical Instrumentation Engineers (SPIE) Conference Series, 990905
Zieleniewski, S., Thatte, N., Kendrew, S., et al. 2015, MNRAS, 453, 3754

Appendix A: Distance estimates for main sequence stars in K_S band

blah blah

Appendix B: Comparison of the HAWK-I and MICADO configuration files

The SimCADO package for Python is in the public domain. We encourage anyone interested in simulating future ELT/MICADO observations to use SimCADO and to report any bugs to the authors. In the interests of transparency and reproducibility, we have included the configuration files that we used to generate SimCADO models of both the HAWK-I and MICADO optical trains. We are also willing to share any of the data files that subsequent users may need in order to reproduce our results. Please contact Kieran Leschinski directly.

Appendix B.1: The MICADO configuration file

The standard configuration file used for the MICADO wide-field (4 mas plate scale) imaging mode.

```
################################################
# Observation Parameters

OBS_DATE                0
OBS_TIME                0
OBS_RA                  90.
OBS_DEC                 -30.
OBS_ALT                 0
OBS_AZ                  0
OBS_ZENITH_DIST         0
OBS_PARALLACTIC_ANGLE   0
OBS_SEEING              0.6

OBS_FIELD_ROTATION      0

OBS_EXPTIME             60
OBS_NDIT                1
OBS_NONDESTRUCT_TRO     2.6
OBS_REMOVE_CONST_BG     no
OBS_READ_MODE           single
OBS_SAVE_ALL_FRAMES     no

OBS_INPUT_SOURCE_PATH   none
OBS_FITS_EXT            0

OBS_OUTPUT_DIR          "./output.fits"


################################################
# Simulation Parameters

SIM_DETECTOR_PIX_SCALE  0.004
SIM_OVERSAMPLING        1
SIM_PIXEL_THRESHOLD     1

SIM_LAM_TC_BIN_WIDTH    0.001
SIM_SPEC_MIN_STEP       1E-4

SIM_FILTER_THRESHOLD    1E-9
SIM_USE_FILTER_LAM      yes
# if "no"
SIM_LAM_MIN             1.9
SIM_LAM_MAX             2.41
SIM_LAM_PSF_BIN_WIDTH   0.1
SIM_ADC_SHIFT_THRESHOLD 1

SIM_PSF_SIZE            1024
SIM_PSF_OVERSAMPLE      no
SIM_VERBOSE             no
SIM_SIM_MESSAGE_LEVEL   3

SIM_OPT_TRAIN_IN_PATH   none
SIM_OPT_TRAIN_OUT_PATH  none
SIM_DETECTOR_IN_PATH    none
SIM_DETECTOR_OUT_PATH   none


################################################
# Atmospheric Parameters

ATMO_USE_ATMO_BG        yes

ATMO_TC                 TC_sky_25.tbl
ATMO_EC                 EC_sky_25.tbl
ATMO_BG_MAGNITUDE       13.6

ATMO_TEMPERATURE        0
ATMO_PRESSURE           750
ATMO_REL_HUMIDITY       60
ATMO_PWV                2.5


################################################
# Telescope Parameters

SCOPE_ALTITUDE          3060
SCOPE_LATITUDE          -24.589167
SCOPE_LONGITUDE         -70.192222

SCOPE_PSF_FILE          scao
SCOPE_STREHL_RATIO      1
SCOPE_AO_EFFECTIVENESS  100
SCOPE_JITTER_FWHM       0.001
SCOPE_DRIFT_DISTANCE    0
SCOPE_DRIFT_PROFILE     linear

SCOPE_USE_MIRROR_BG     yes

SCOPE_NUM_MIRRORS       5
SCOPE_TEMP              0
SCOPE_M1_TC             TC_mirror_EELT.dat
SCOPE_MIRROR_LIST       EC_mirrors_EELT_SCAO.tbl


################################################
# Instrument Parameters

INST_TEMPERATURE        -190

INST_ENTR_NUM_SURFACES  4
INST_ENTR_WINDOW_TC     TC_window.dat

INST_DICHROIC_NUM_SURFACES  2
INST_DICHROIC_TC        TC_dichroic.dat
```

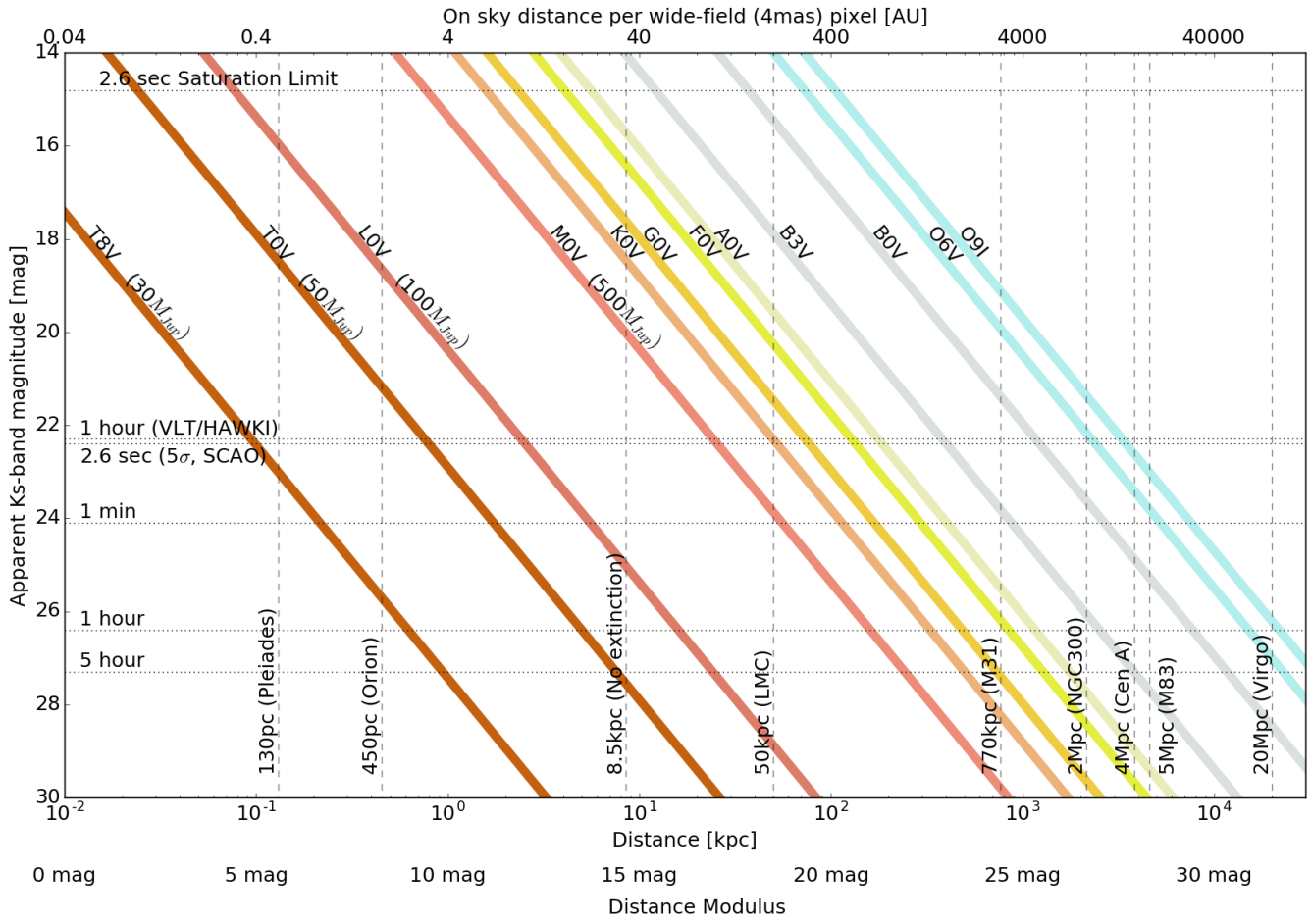

Fig. .1. The Ks-band equivalent of Figure 5.3

```
INST_FILTER_TC          Ks

INST_PUPIL_NUM_SURFACES 2
INST_PUPIL_TC           TC_pupil.dat

# MICADO, collimator 5x, wide-field 2x (zoom 4x)
INST_NUM_MIRRORS        11
INST_MIRROR_TC          TC_mirror_gold.dat

INST_USE_AO_MIRROR_BG   yes
INST_AO_TEMPERATURE     0
INST_NUM_AO_MIRRORS     7
INST_MIRROR_AO_TC       TC_mirror_gold.dat
INST_MIRROR_AO_LIST     EC_mirrors_ao.tbl

INST_ADC_PERFORMANCE    100
INST_ADC_NUM_SURFACES   8
INST_ADC_TC             TC_ADC.dat

INST_DEROT_PERFORMANCE  100
INST_DEROT_PROFILE      linear

INST_DISTORTION_MAP     none
INST_WFE                data/INST_wfe.tbl
INST_FLAT_FIELD         none
```

```
################################################
# Spectroscopy parameters

SPEC_ORDER_SORT         HK
SPEC_SLIT_WIDTH         narrow

################################################
# Detector parameters

FPA_USE_NOISE           yes

FPA_READOUT_MEDIAN      4
FPA_READOUT_STDEV       1
FPA_DARK_MEDIAN         0.01
FPA_DARK_STDEV          0.01

FPA_QE                  TC_detector_H2RG.dat
FPA_NOISE_PATH          FPA_noise.fits
FPA_GAIN                1
FPA_LINEARITY_CURVE     FPA_linearity.dat
FPA_FULL_WELL_DEPTH     1E5

FPA_PIXEL_MAP           none
# if FPA_PIXEL_MAP == none
FPA_DEAD_PIXELS         1
FPA_DEAD_LINES          1
```

```
FPA_CHIP_LAYOUT         full
FPA_PIXEL_READ_TIME     1E-5
FPA_READ_OUT_SCHEME     double_corr

################################################
# NXRG Noise Generator package parameters
# See Rauscher (2015) for details
# http://arxiv.org/pdf/1509.06264.pdf

HXRG_NUM_OUTPUTS        64
HXRG_NUM_ROW_OH         8
HXRG_PCA0_FILENAME      FPA_nirspec_pca0.fits
HXRG_OUTPUT_PATH        none
HXRG_PEDESTAL           4
HXRG_CORR_PINK          3
HXRG_UNCORR_PINK        1
HXRG_ALT_COL_NOISE      0.5

HXRG_NAXIS1             4096
HXRG_NAXIS2             4096
HXRG_NUM_NDRO           1
```

Appendix B.2: The HAWKI configuration file

Rather than listing the full configuration for SimCADO as in B.1, we simply list the parameters that were changed in order to create an optical train for UT4/HAWKI at the VLT.

```
#####################################
# Parameters regarding the "observation"

OBS_RA                  245.885625
OBS_DEC                 -26.53835
OBS_SEEING              0.6

OBS_EXPTIME             10
OBS_NDIT                1

#####################################
# Parameters relating to the simulation

SIM_DETECTOR_PIX_SCALE  0.106


#####################################
# Parameters regarding the telescope

SCOPE_ALTITUDE          2635
SCOPE_LATITUDE          -24.589167
SCOPE_LONGITUDE         -70.192222

SCOPE_PSF_FILE          PSF_HAWKI_poppy.fits

SCOPE_NUM_MIRRORS       3
SCOPE_M1_TC             TC_mirror_aluminium.dat
SCOPE_MIRROR_LIST       EC_hawki_vlt_mirrors.tbl


#####################################
# Parameters regarding the instrument

INST_TEMPERATURE        -130

INST_ENTR_NUM_SURFACES  4
INST_FILTER_TC          TC_filter_Ks_HAWKI.dat
INST_PUPIL_NUM_SURFACES 2

INST_NUM_MIRRORS        4
INST_MIRROR_TC          TC_hawki_mirror.dat

INST_USE_AO_MIRROR_BG   no
INST_AO_TEMPERATURE     0
INST_NUM_AO_MIRRORS     0

INST_ADC_PERFORMANCE    0
INST_ADC_NUM_SURFACES   0
INST_ADC_TC             none

INST_WFE                INST_hawki_wfe.tbl


#####################################
# General detector parameters

FPA_READOUT_MEDIAN      12
FPA_QE                  TC_hawki_H2RG.dat
FPA_LINEARITY_CURVE     FPA_hawki_linearity.dat
FPA_CHIP_LAYOUT         FPA_hawki_layout_cen.dat


########################################
# NXRG Noise Generator package parameters
# See Rauscher (2015) for details
# http://arxiv.org/pdf/1509.06264.pdf

HXRG_NUM_OUTPUTS        32
HXRG_NUM_ROW_OH         8
```